Aus dem Julius-Wolff Institut
der Medizinischen Fakultät Charité – Universitätsmedizin Berlin

DISSERTATION

Influence of physical cues from the degrading magnesium implants on human cells

Einfluss der *Physical Cues* der degradierenden Magnesiumimplantate auf humane Zellen

zur Erlangung des akademischen Grades

Doctor of Philosophy (PhD)

vorgelegt der Medizinischen Fakultät
Charité – Universitätsmedizin Berlin

von

Romina Amberg

aus Berlin

Datum der Promotion: 05.03.2021

Table of Contents

Abstract

Magnesium, as a biodegradable and biocompatible metal implant material for the orthopedic and vascular application, is also very promising in guided bone regeneration (GBR) to treat periodontal defects in dentistry. Therefore, thin magnesium membranes could replace the currently used barrier membranes made of resorbable collagen or non-resorbable titanium-reinforced polytetrafluorethylene (PTFE) for bone augmentation. Non-resorbable membranes are often reported to lead to exposed membranes as a result of postoperative wound dehiscence, and are accompanied by an increased infection risk and an extended healing period. Migration of human gingival fibroblasts (HGF) on the barrier membranes can overcome the exposed membrane by forming a cellular monolayer, which allows endothelial cells to finally close the wound. A migration assay has been developed during my previous research to investigate migration behaviour *in vitro* on magnesium surfaces. This study revealed that migration of HGF was slower on magnesium than on titanium and tissue culture plastic as control surfaces. During migration on magnesium, the cells were exposed to the alteration of various parameters, so called 'physical cues', involving surface alterations due to the formed corrosion layer and medium alterations arising from the dissolved corrosion products. Surface analysis by atomic force microscopy (AFM), scanning electron microscopy (SEM) and wettability measurements of all used materials revealed that the surface can be excluded as a parameter affecting migration rate on magnesium. Therefore, the main part of this study focused on analyzing the effect of the physical cues arising from the medium, like increasing Mg^{2+}, H_2 and osmolality as well as decreasing Ca^{2+} on HGF, including migration, viability and proliferation studies. It was shown that the altered ratio of Mg^{2+} and Ca^{2+}, caused by increasing Mg^{2+} and decreasing Ca^{2+} concentration, accompanied by an increase of H_2 concentration resulting from magnesium corrosion, led to reduced migration rate of HGF on magnesium surfaces. Furthermore, the individual increase of Mg^{2+} concentration up to 25 mM did not affect migration behaviour of HGF, while the migration rate decreased with decreasing Ca^{2+} concentration from 1.16 to 0 mM. This study provides detailed results of physical cues from the degrading magnesium membranes affecting migration, proliferation and viability of HGF. This knowledge allows us to create optimal conditions for the clinical application of magnesium membranes to ensure optimal healing success.

Zusammenfassung

Magnesium, als ein metallisches Imlantatmaterial für die orthopädische und vaskuläre Anwendung eignet sich aufgrund seiner Biodegradierbarkeit und Biokompatibilität hervorragend für die Anwendung in der gesteuerten Knochenregeneration (eng. Guided Bone Regeneration, GBR) zur Behandlung von parodontalen Defekten in der Zahnheilkunde. In Form von dünnen Membranen kann Magnesium die derzeit für den Knochenaufbau eingesetzten Barrieremembranen, bestehend aus resorbierbaren Kollagen oder nicht-resorbierbaren Titan verstärkten Polytetrafluorethylen (PTFE), ersetzen. Nicht-resorbierbare Barrieremembranen haben den Nachteil, dass häufig postoperative Wunddehiszenzen auftreten, währenddessen die Membran freigelegt wird, wodurch das Infektionsrisiko steigt und die Heilungsphase verzögert wird. Durch Migration von humanen gingivalen Fibroblasten (HGF) auf der Membran bildet sich ein zellulärer Monolayer, auf dem letztendlich die Endothelzellen migrieren können, um die offene Wunde zu schließen. Im Rahmen meiner bisherigen Forschungsarbeit habe ich einen Migrationsassay entwickelt, mit dem sich das Migrationsverhalten von Zellen *in vitro* auf Magnesiumoberflächen untersuchen lässt. Die Studie zeigt, dass die HGF auf der Magnesiumoberfläche langsamer migrieren, als auf der Titan- und der Kunststoffoberfläche, es aber dennoch zu einem Wundverschluss kommt. Infolge der Korrosion von Magnesium ändern sich die Umgebungsparameter, denen die Zellen während der Migration auf Magnesium ausgesetzt sind. Das sind zum einen Veränderungen im Medium durch gelöste Korrosionsprodukte und zum anderen Veränderungen der Magnesiumoberfläche aufgrund der Bildung einer Korrosionsschicht. Parameter, mit denen sich diese Veränderungen charakterisieren lassen, werden als ‚physical cues' bezeichnet.

Oberflächenanalysen mittels Rasterkraftmikroskopie, Rasterelektronenmikroskopie und Messungen zur Bestimmung der Benetzbarkeit zeigten, dass die Oberfläche keinen Einfluss auf die Migrationsrate der HGF auf den Magnesiummembranen hat. Demzufolge wird angenommen, dass nur die physical cues, mit denen sich das Medium charakterisieren lässt einen Einfluss auf das Zellverhalten haben. Auf dieser Annahme basierend, liegt der Fokus der Arbeit, insbesondere auf der Untersuchung der Auswirkungen einer gesteigerten Mg^{2+} Konzentration, H_2 Konzentration und Osmolalität sowie abnehmender Ca^{2+} Konzentration auf die Migration, Viabilität und Proliferation der HGF. Die Ergebnisse zeigten, dass sich die verlangsamte Migration der HGF auf Magnesium mittels der korrosionsbedingten Veränderung des Verhältnisses von Mg^{2+}

und Ca^{2+}, sowie der gesteigerten H_2 Konzentration im Medium erklären lässt. Darüber hinaus hat der alleinige Anstieg von Mg^{2+} im Medium auf bis zu 25 mM keinen Einfluss auf die Migrationsrate der HGF, während die alleinige Abnahme der Ca^{2+} Konzentration von 1,16 zu 0 mM eine verlangsamte Migration zur Folge hat. Die Studie liefert detaillierte Ergebnisse über die Auswirkungen der physical cues der Magnesiummembranen auf das Zellverhalten der HGF hinsichtlich Migration, Viabilität und Proliferation. Mit diesem Wissen lassen sich optimale Bedingungen für die klinische Anwendung der Magnesium-Membranen schaffen, um einen optimalen Heilungserfolg anzustreben.

1 Introduction

Since the last century, magnesium-based implants have been probed in many studies for orthopedic and cardiovascular applications [1]. In contrast to other metal implants, magnesium is completely biodegradable by forming magnesium ions, molecular hydrogen and hydroxide ions in physiological conditions; hence, there is no need for a second surgery for implant removal [1]. Another advantage of magnesium is its biocompatibility due to magnesium ions being the 4th abundant cations in the human body and being involved as co-factors in numerous physiological reactions [1, 2].

Beside their biocompatibility and biodegradability, magnesium shows low elastic moduli similar to natural bone, thus preventing stress shielding of the regenerating bone [3]. Stress shielding occurs when the implant bears the mechanical load and relieves the healing bone, leading to delayed bone regeneration and in the worst case resulting in bone resorption [3].

Due to its excellent properties, magnesium could also be used in form of thin membranes for the guided bone regeneration (GBR) in dentistry to treat periodontal bone defects for inserting implant abutments [4]. As a first step of the GBR treatment, the defective bone is filled with bone substitute and the dental implant is inserted [5]. As a next step, the regenerating bone is covered by a barrier membrane, which is dressed by gingival tissue [5]. The GBR membrane provides a space for bone substitute replacement by natural bone and prevents ingrowth of the adjacent gingival tissue for optimal healing success [5].

Due to their excellent biodegradability and biocompatibility, currently used GBR-membranes are often made of collagen when simple bone augmentation is required [5]. In case of bone defects including alveolar wall defects, a barrier membrane with high volume stability is required. A current solution is non-resorbable titan-reinforced PTFE membranes, which provide high volume-stability due to its excellent mechanical stiffness [5]. However, the missing biodegradability requires a second surgery for implant removal after bone regeneration is completed, which is associated with a high burden for the patient, such as an extended healing period [5].

In this context, magnesium-based membranes combine adequate mechanical strength with the advantage of resorbability, which make magnesium a very promising implant material for GBR-membranes. Moreover, the reported antibacterial properties and the osteoproliferative effects of magnesium, resulting from the release of magnesium ions

and hydroxide ions during magnesium corrosion, provide a great advantage compared to the current used membranes [6, 7]. In regard to non-resorbable GBR-membranes based on titanium, membrane exposure (Fig.1) provoked by insufficient tissue coverage for primary wound closure or wound dehiscence during healing is often reported as the main problem of non-resorbable membranes due to the high infection risk [8]. Wound dehiscence arise in 31% of all GBR procedures using non-resorbable GBR-membranes, resulting in early membrane removal associated with an decreased regeneration rate (0-60%) [9]. An exposed membrane can be overcome by migration of human gingival fibroblasts (HGF) on the GBR membrane to form a cellular monolayer, which allows epithelial cells to migrate to the top of the HGF to finally close the wound [10].

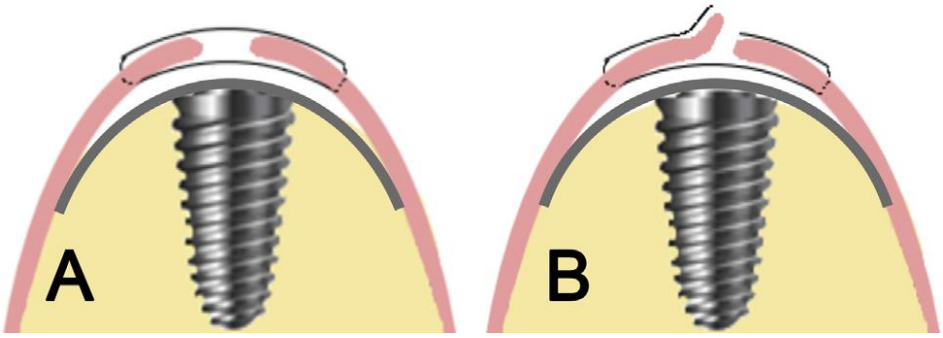

Figure 1. Membrane exposure due to incomplete soft tissue coverages after surgery (A) or due to wound dehiscence (B) [4].

This clearly demonstrates the high relevance of investigating the migration behaviour of HGFs on GBR-membranes, especially on magnesium as a novel membrane material. During my previous research, I developed a scratch-based migration assay on magnesium membranes, including fluorescent cell staining and pre-corrosion of magnesium, which allows studying wound closure of HGF *in vitro* on biodegradable magnesium under life view conditions [4]. The results showed that migration is slower on magnesium surfaces than on tissue culture plastic surfaces. To obtain more reliable results, current used membrane materials such as titanium surfaces should be tested with the established migration assay to compare the migration behaviour. Furthermore, during cell migration on magnesium membranes, the HGF are affected by the medium alterations arising from the dissolved corrosion products and by surface alteration due to the formation of a corrosion layer. All parameters characterizing the environmental parameter and the surface properties of a material are so called ‘physical cues’. Each physical cue affects cell proliferation, viability and migration of HGF and needs to be

considered in the clinical application of magnesium membranes. In regard to medium alteration, the magnesium ions concentration, osmolality, pH value and molecular hydrogen concentration increase [11], and calcium ion concentration decreases [12] due to magnesium corrosion. The surface condition can be characterized by wettability, roughness and topography measurements. Therefore, the current study included surface characterization of magnesium, as well as titanium and tissue culture plastic as control surfaces by using atomic force microscopy, electron scanning microscopy and wettability measurements.

The investigation of physical cues from degrading magnesium affecting HGF, especially cell migration, offers new opportunities for the clinical application of magnesium membranes for the GBR and is needed for ensuring optimal healing success. Moreover, cell migration is essential in any regeneration processes and particularly on implanted device surfaces, emphasizing the high relevance for migration studies on magnesium membranes as a novel implant material.

Hence, the aim of this study was to analyze migration behaviour of HGF on magnesium membranes by investigating the physical cues from the degrading magnesium and their separate effect on cell migration, proliferation and viability.

2 Methods

2.1 Cell culture

All experiments were performed with human gingival fibroblasts (HGF-1 CRL-2014, ATCC, Manassas, USA), which were cultivated in cell culture medium (CCM) under cell culture conditions (37 °C, 20% O_2, 5% CO_2, 95% rH) in a Hera-cell240 incubator (Heraeus, Hanau, Germany). The CCM consists of phenol red free Dulbecco's modified Eagle medium (DMEM)/F-12, penicillin/streptomycin (100 U ml-1, 100 µg ml-1) (both Life Technologies GmbH, Karlsruhe, Germany) and 10% fetal bovine serum superior (FBS, Biochrom GmbH, Berlin, Germany). At 80-90% confluence under the DMIL microscope (Leica, Wetzlar, Germany), the cells were splitted in new cell culture flasks (Sarstedt Nürnbrecht, Germany) by rinsing the cells with phosphate buffered saline solution (PBS, Life Technologies GmbH), and were then detached with trypsin (0.25% Trypsin-EDTA solution, Sigma-Aldrich, Steinheim, Germany) for 2 min. Cell refeeding with fresh CCM ensued every 2-3 days.

2.1 Migration assay

To compare the migration behaviour of human gingival fibroblasts (HGF) on magnesium membranes (Botiss biomaterials GmbH, Berlin, Germany, Purity: 99.95%, 13 x10 mm, thickness: 140 µm) with them on current used non-resorbable GBR-membranes, the established migration assay, which is described in my paper [4] was performed on gamma-sterilized titanium discs (Goodfellow, Friedberg, Germany, Purity: 99.6%, Ø15 mm, thickness: 140 µm). The migration curve, obtained from the evaluated images using the software Tscratch, represents the averaged cell free area of six replica as a function of the time.

2.2 Surface characterization

The roughness and topography of uncorroded and 72 h pre-corroded gamma-sterilized magnesium membranes, which were used for the migration assay, were already determined during my previous research [4]. The analysis was completed by roughness measurements with the atomic force microscopy (AFM) of titanium discs and tissue culture plastic (TCP, 24-well plate, Sarstedt, Nürnbrecht, Germany) and topography

images of titanium discs using the scanning electron microscopy (SEM). Additionally, the wettability was determined for magnesium (uncorroded and pre-corroded), titanium discs and TCP. The utilized surface methods are described in the following sections.

2.2.1 Topography - Scanning electron microscopy (SEM)

In contrast to light microscope, the scanning electron microscope (SEM) uses electrons for imaging, whereby a magnification of up to 10^5 x and a resolution of 1-5 nm can be achieved [13]. The high depth of sharpness and the high magnifications of the SEM allow capturing of high-resolution topography images. Samples need to be electrically conductive and resistant to vacuum. Non-conductive sample can be made electrically conductive by coating with a thin gold layer in a sputtering process [14]. But, there are already modern SEM working with low vacuum to investigate non-conductive samples without sputtering [15].

An electron gun generates a beam of electrons by thermal emission (Fig.2) [14]. The electrons dissolve from the cathode and were accelerated to the anode under vacuum. The acceleration voltage determines the energy of the electrons leaving the anode, which is between 2-30 keV [14]. Operating under vacuum avoids electrons to collide with gas molecules and allows using the wave properties of electrons [16]. Electrons were focused by the condenser lens to a small electron beam, which is scanned in a raster pattern over the sample surface [14]. Scanning is achieved by the beam deflector containing scanning coils. When electrons hit the sample, they interact elastically or inelastically with the sample atoms [17]. During elastically interaction, the electron is scattered by the positive atom nucleus. The generated backscattered electrons (BSE) are characterized by a low energy loss and were detected with a semiconductor detector [17]. Inelastically interaction occurs when the impinging electron knocks another electron from its atomic shell, which is called secondary electron (SE) [17]. Secondary electrons (SE) show a high energy loss with a high deflection angle and are detected with the Everhart-Thornley detector, a type of scintillation-photomultiplier system [17]. The detector signal is amplified and converted in an indirect image on the screen. Every voltage signal is assigned to a brightness value. Topography images are principally captured using SE-signals, whereas BSE signals provide information about the chemical composition of the sample [14]. Although SE are generated in the whole sample, the generated SE in deeper layers cannot escape the sample due to their low energy and are thus absorbed.

Therefore, only the SE in direct vicinity to the interface form the signal (escape depth for metals: 5 nm and for isolators: 50 nm), which are 1% of all formed SE [18].

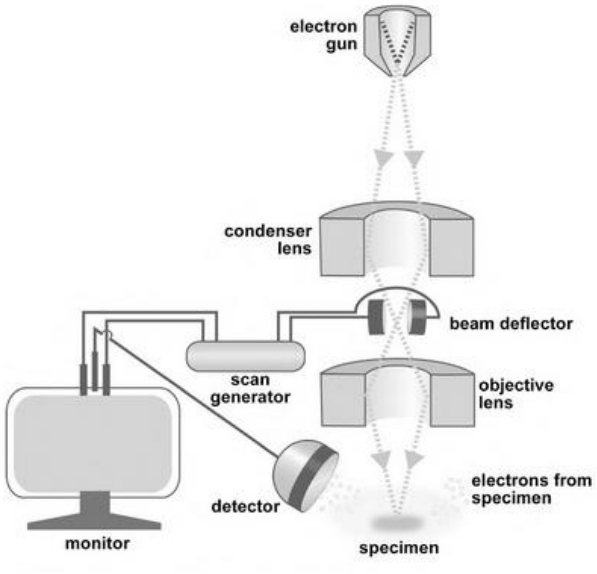

Figure 2. The basic components of the scanning electron microscope (SEM) [17].

Nontheless, these SE signals create high-resolution images of the topography of the sample surface. An elevated point of the surface leads to forming a higher SE amount, resulting in a higher voltage signal [18]. The higher the voltage signal, the brighter the pixel captured in the image [18]. The titanium discs were measured with the SEM JCM-6000Plus NeoScope™ (Joel, Tokyo, Japan) operating with the high vacuum mode at an acceleration voltage of 5 kV using the SE signals to image the topography of the titanium surface.

2.2.2 Roughness - Atomic force microscopy (AFM)

The atomic force microscopy (AFM) enables roughness measurements of micro- and nanostructures by imaging topographical profiles [19]. The mean roughness R_a is the most common surface roughness parameter, and is the arithmetic averaged height of roughness-component irregularities from the mean line, measured within the sampling length l_r (Fig.3) [20].

$$R_a = \frac{1}{l_r}\int_0^{l_r} |z(x)|\, dx \qquad (1)$$

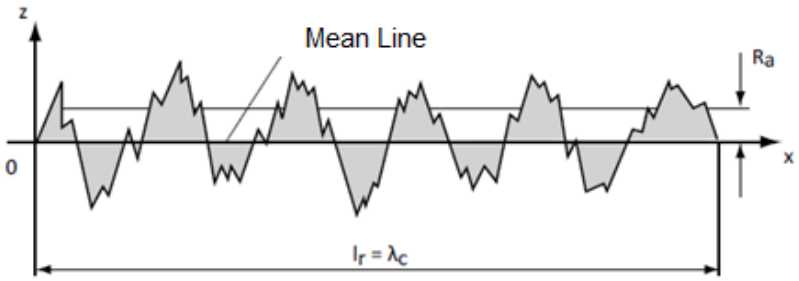

Figure 3. Mean roughness R_a for a roughness profile [21].

Further 2D parameters are the mean roughness depth R_z and the root mean square R_q [22], which are all obtained from a single line of the surface. The 3D parameters S_a, S_q and S_z, are used for characterization of defined area, and are the averaged value of all line profiles [22].

The measuring principle is based on scanning a surface with a very sharp tip, which is fixed on a cantilever using the interactions between a tip and a sample surface to get a topographical image of the sample surface [23]. The sample is moved in the x, y and z directions by a piezoelectric material, thus position can be controlled in nanometer resolution [24]. The tip is generally made of silicon (Si), silicon nitride (Si_3N_4) or silicon dioxide (SiO_2) with a contact radius of several nm up to 100 nm [25]. A laser beam is focused onto the back of the cantilever and is reflected back to a photodiode detector (Fig.4). Depending on the atomic force variations between the tip and the sample surface, the deflection of the cantilever can be measured precisely and detected as a topographical image.

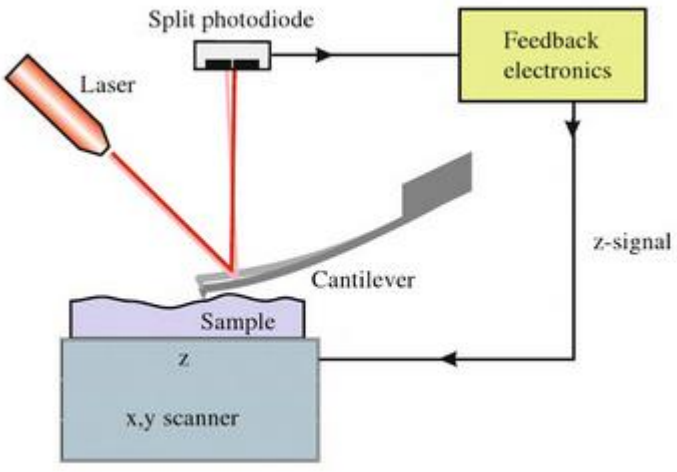

Figure 4. Schematics of atomic force microscopy (AFM) operation [24].

There are two operation modes: the contact mode and the non-contact mode depending on whether the tip touches the surface during the measurement. In the contact mode, the signal can be set to a constant height (constant height mode) or a constant force (constant force mode) of the cantilever [23]. When operating in constant height mode, the tip scan the surface, while the cantilever bends and supplies a signal to the detector [23, 24]. Maintenance of constant force between the tip and the cantilever (constant force mode) is achieved using a control loop to obtain a constant photodiode signal [23, 24]. The feedback signal of the control loop contains information of the surface topography [23]. The contact mode has a high resolution and a fast measurement time; the disadvantages are that the lateral resolution is limited due to the diameter of the tip and that the sample can be destroyed, thus modified results may be obtained [24].

The disadvantages of the contact mode were the reason for developing the non-contact mode in 1987 by Martin *et al.* [23]. In the non-contact mode the cantilever oscillates at its resonance frequency in a distance of 10-100 nm from the surface [23, 25]. Variations in the distance between the surface and the tip lead to alter the resonance frequency or vibration amplitude [19, 26]. On the one hand, the frequency alteration can be measured at constant amplitude (FM-AFM); on the other hand, the amplitude alteration can be measured at constant frequency (IC-AFM) [26]. Therefore, the respective measurement variable feeds the control loop.

The titanium and tissue culture surfaces were measured in the non-contact mode (IC-AFM) with the atomic force microscope easyScan 2 (Nanosurf®, Liestal, Switzerland). The tip was made of silicon and had a contact diameter of 7 nm (Nanosensors Typ PPP-NCLR-10, Switzerland). The 3D mean roughness values S_a were determined using the software Gwyddion 2.45.

2.2.3 Wettability measurements

The wettability describes the relative adhesion of a liquid such as water or a solvent to a solid surface due to intermolecular interactions [27]. The contact angle measurement is a common method used to determine the wettability of a surface. Therefore, the contact angle θ between the sessile drop and the sample surface is measured. Contact angles less than 90° reveal wettable surfaces, while contact angles above 90° were obtained for non-wettable surfaces (Fig.5). In cases where water is used to wet the surface,

hydrophilic surfaces have contact angles less than 90° and hydrophobic surfaces above 90°.

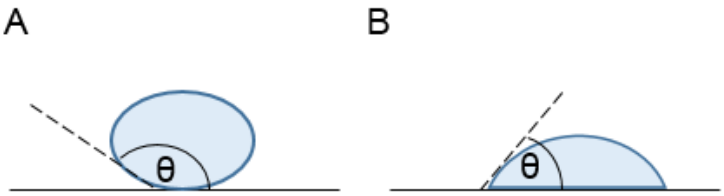

Figure 5. Contact angle above 90° (A) and below 90° (B).

The surface free energy (SFE, σ_s) is the surface tension of a solid and can be determined by measuring the contact angle of more than one liquid using the model of Owens, Wendt, Rabel and Kaelble (OWRK-model) [28, 29], which is based on the Young equation.
The Young equation describes the relationship between the surface free energy σ_s of the sample surface, the interfacial tension σ_{sl} between liquid and solid, the surface tension σ_l of the liquid and the contact angle θ [27]:

$$\sigma_s = \sigma_{sl} + \sigma_l \cdot \cos\theta \qquad (2)$$

In contrast to the wettability, described by a contact angle of one liquid, the SFE is independent of the liquid used. One can predict the behaviour of any liquid on the surface by knowing the SFE.
In our case, the contact angles of water and diiodomethane were measured on titanium, magnesium (pre-corroded, uncorroded) and tissue culture plastic (TCP) surfaces using the Drop Shape Analyzer DSA 25 (Krüss GmbH, Nürnberg, Germany) with the sessile drop method. The SFE were calculated from the measured water contact angle (θ_{water}, WCA) and diiodomethane contact angle ($\theta_{diiodom.}$, DCA) and the surface tension of the liquids (σ_{water} = 72.8 mN m^{-1}, $\sigma_{diiodom.}$ = 50.8 mN m^{-1}) using the equation (2).

2.3 Modified migration assay

The established migration assay allows migration studies directly on non-transparent surfaces. To verify whether surface alterations of magnesium surface affects cell migration, the migration assay was modified. To exclude the direct surface contact of the cells to the pre-corroded magnesium membrane, the HGF were seeded on the bottom of the 24-well plate and affected by the corroding magnesium membranes, at a distance of 2 mm from the cells. In accordance with the established migration assay, the utilized magnesium membrane was pre-corroded for 72 h in 10 mL CCM in a tightly closed 15 mL falcon tube (Becton & Dickinson, Heidelberg, Germany) on a roll mixer (Phoenix,

Garbsen, Germany) under cell culture conditions. After labeling the HGF with 10 mM fluorescent dye CellTracker™ Red CMTPX (Life Technologies GmbH) for 30 min using serum free CCM, the cells were cultured for 24 h in CCM, before cell seeding ($4 \cdot 10^4$ cell/ 1 mL/ well) into the silicone inserts ($Ø_{inner}$: 10 mm) of the 24-well plate. The silicone inserts fit precisely into the wells of the plate and were made of transparent autoclavable casting compound of silicon elastomer (Sylgard® 184, Sigma-Aldrich, Steinheim, Germany). Cells were allowed to adhere for 24 h. To ensure conditions comparable to the established migration assay, the pre-corroded magnesium membrane was also incubated with 1 mL CCM for 24 h. After removing the silicone inserts, the confluent cell monolayer was scratched with a sterile pipette tip (10 µL), rinsed with serum free CCM, and the pre-corroded magnesium membrane was placed on a silicone half ring identical to the original assay with the only difference being that the cells do not grow on the magnesium membrane but on the plastic bottom.

The silicone half rings ($Ø_{inner}$: 10 mm, $Ø_{outer}$: 14 mm, thickness: 2 mm) were generated by stamping the autoclavable silicone sheet (Exact Plastics GmbH, Bröckel, Germany) and creating four tunnels to ensure optimal medium exchange. The set-up was completed by adding 2 mL CCM to the cells and fixing the membrane with two glass stones, respectively. The plate was incubated for 4 h under cell culture conditions and then tipped in a 45° angle before the 72-h imaging period began. This step was crucial to remove the newly formed hydrogen bubbles due to highly initial corrosion rate of magnesium, which would impair the imaging. The images were taken every 5 h using the DMI6000 B inverted fluorescent microscope (Leica, Mannheim, Germany) with a live cell imaging system and evaluated with the software TScratch (see 2.1).

The cell migration behaviour on magnesium (Mg-direct) from the previous experiments [4] were compared to them, which were only affected by the corroding medium (Mg-indirect).

2.4 Characterization of the supernatants during cell migration

Both migration assays (Mg-direct, Mg-indirect) were performed and the hydrogen concentration of the supernatant was measured with the Hydrogen Microsensor Multimeter (Unisense, Aarhus, Denmark) at starting point (0 h), after 25 h and after 50 h, by measuring each sample for 30 s without stirring. The supernatants were removed and stored at -20 °C for several days until shipping on dried ice to Freiberg University of

Mining and Technology (Germany) for further investigations. The quantification of Mg^{2+} and Ca^{2+} was determined by inductively coupled plasma optical emission spectrometry (ICP-OES) using an iCAP 6000 from Thermo Fisher Scientific (Bremen, Germany) with an Echelle grating optical system and a Charge Injection Device (CID), type CID86 detector. Nebulizer was PEEK (Polyetheretherketon) MiraMist (Burgener, Mississauga, Canada). Method parameters were the following: Rf power 1100 W; radial viewing plasma mode; coolant gas flow 12.0 L min^{-1}; auxiliary gas flow 0.6 L min^{-1}; nebulizer gas flow 0.65 L min^{-1}. Sample digestions were prepared with 2% nitric acid made of ultrapure deionized water with a conductivity of 0.055 µS/cm, obtained from MicroPure water purification system from TKA (Niederelbert, Germany), and nitric acid from Merck KgaA (Darmstadt, Germany) that was bidistilled in-house with PFA sub-boiling acid distillation system DST-100 from AHF Analysentechnik AG (Tübingen, Germany). For quantification, external calibration models with dilutions of stock solutions from Merck KgaA were used. Emission lines 279.55 nm, 280.27 nm and 285.21 nm for magnesium and emission line 396.85 nm for calcium were measured and evaluated.

The osmolality and pH value of the supernatants after migration on magnesium membranes (Mg-direct) were determined by previous research [4].

2.5 Ca^{2+} determination in the corrosion layer of Mg membranes

While performing the unmodified migration assay (Mg-direct), the magnesium membranes were removed at starting point (0 h), after 25 h and after 50 h and stored at -20 °C for several days until shipping on dried ice to Freiberg University of Mining and Technology, for Ca^{2+} determination. After digestion of each Mg membrane with 1 mL nitric acid (69%), the samples were diluted with ultrapure deionized water and measured with ICP-OES.

2.6 Immunohistological analysis

The effect of increasing Mg^{2+} in the medium on cell adhesion of HGF was investigated by immunohistological staining. Therefore, the HGF were seeded in a 48-well plate ($4 \cdot 10^4$ cells/well) and allowed to adhere for 24 h. Then, the cells were incubated with 25 mM and 75 mM $MgCl_2 \cdot 6\,H_2O$ for 24 h, rinsed with serum free CCM, and fixed with polymeric formaldehyde (PFA) for 10 min (400 µL/well). Cells were rinsed three times for 3 min with TRIS-buffered solution (TBS) washing buffer (pH 8.2, 0.025% Triton) and permeabilized

with 0.25% Triton in TBS (pH 8.2) for 10 min. After washing with TBS washing buffer, the cells were treated with blocking solution for 30 min to block unspecific bindings to the substrate. The blocking solution contained 5% goat serum and 1% BSA (bovine serum albumin) in TBS (pH 8.2, without Triton) (both Abcam, Cambridge, UK). Then, the blocking solution was removed and the cells were incubated with the Anti-Vinculin mouse antibody (Merck, Darmstadt, Germany) for 17 h at 4 °C, which was diluted 1:150 with antibody diluent (Merck) (150 µL/well). The antibody solution was removed and the cells were rinsed three times for 5 min with TBS washing buffer. Cells were incubated with a mixture of the goat Anti-mouse lgG Alexa Fluor® 488 secondary antibody (1:400 dilution) and Alexa Fluor® 594 Phalloidin (1:100 dilution) (both Thermo fisher scientific Molecular Probes, Waltham, USA) in TBS (pH 8.2, without Triton) for 1 h, containing additionally 1% BSA and 5% goat serum (150 µL/well). The incubation was performed in the dark. After rinsing the cells three times for 5 min with TBS washing buffer and once with sterile injection water (B Braun, Penang, Malaysia), the cell nucleus was stained with 4′,6-Diamidin-2-phenylindol (DAPI, 1:1500 dilution with sterile injection water) by incubating for 15 min. After removing DAPI, the well plate was stored at 4 °C, containing TBS washing buffer until imaging was performed with the Axio Observer fluorescence microscope (Zeiss, Jena, Germany).

2.7 Preparing test solutions

To investigate the effect of increasing Mg^{2+} and osmolality, as well as decreasing Ca^{2+} concentration on cell behaviour, various saline solutions including controls were prepared. Increased hydrogen concentration was implemented by enriching cell culture medium with molecular hydrogen. The effect of pH rising was not separately tested, as previous experiments showed that pH does not increase significantly during migration on magnesium implants due to the buffered system [4]. The combined effect of all altered physical cues during magnesium corrosion on cells was tested by preparing various magnesium extracts.

Saline Solutions

Cell culture medium (CCM) was supplemented with magnesium chloride hexahydrate ($MgCl_2 \cdot 6\ H_2O$), mannitol and sodium chloride (NaCl), respectively. The concentrations

are declared in Table 1. Mannitol and NaCl were used as controls, as mannitol matches the osmolality and NaCl the chloride concentration, which have to be considered by adding $MgCl_2 \cdot 6\,H_2O$ to the CCM. Additionally, test solutions with different Mg^{2+} concentrations were prepared, which all show same ionic strength and osmolality, achieved by adding various amounts of mannitol and NaCl to the magnesium test solutions. The effect of lower calcium ion concentration was investigated using calcium and phenol free Dulbecco's modified Eagle medium (DMEM, United States Biological, Salem, USA), which was supplemented with 10% FBS and calcium chloride dihydrate ($CaCl_2 \cdot 2\,H_2O$) (Tab.1). All utilized substances were provided by Merck (Darmstadt, Germany), and the prepared solutions were sterile filtrated with the Millex-GV (0.22 µm).

Table 1. Analysis of tested saline solutions and magnesium extracts [4].

		Mg^{2+} [mM]	**Cl^- [mM]**	**Ionic strength [mM]**	**Osmolality [mOsmol Kg^{-1}]**	**Ca^{2+} [mM]**
control	CCM*	0.7	124	---	315±6	1.16
saline solution**	25mM $MgCl_2$	25	50	75	369±6	---
	75mM $MgCl_2$	75	150	225	480±5	---
	Mannitol-1	0	0	0	369±6	---
	Mannitol-2	0	0	0	480±5	---
	50mM NaCl	0	50	50	406±2	---
	150mM NaCl	0	150	150	580±8	---
	0 mM Mg^{2+}	0	75	75	450±3	---
	15 mM Mg^{2+}	15	60	75	450±3	---
	25 mM Mg^{2+}	25	50	75	450±3	---
	0 mM Ca^{2+}	0.7	0	---	307±1	0
	0.3 mM Ca^{2+}	0.7	0	---	308±1	0.3
	0.5 mM Ca^{2+}	0.7	0	---	309±1	0.5
	0.8 mM Ca^{2+}	0.7	0	---	310±1	0.8
Mg-extract	w/o CO_2	4.5±0.1	---	---	330±3	0.93±0.02
	w CO_2	58.2±0.8	---	---	385±3	0.57±0.01

*Cell culture medium

**Values of Mg^{2+}, Ca^{2+}, Cl^- and ionic strength are calculated values and do not include the absolute concentration of the cell culture medium.

Mg-extracts

Mg-extracts were obtained by immersion a magnesium membrane in 10 mL CCM in a 15 mL falcon tube and leaving on a roll mixer for 72 h under cell culture conditions. To obtain two different Mg-extracts, one tube was tightly closed to avoid environmental exchange and another tube was provided with a sterile filter, which was attached to the lid of the tube to ensure environmental exchange. The Mg^{2+} and Ca^{2+} concentrations were determined at Freiberg University of Mining and Technology with ICP-OES (Tab.1). The osmolality of all tested saline solutions and Mg-extracts were determined in triplicate with the osmometer (Gonotec, Berlin, Germany) and are indicated in Table 1.

Hydrogen-rich cell culture medium (H-CCM)

Cell culture medium (CCM) was enriched with molecular hydrogen using the Highdrogen Age_2 Go hydrogen generator (Aquacentrum, München, Germany). Hydrogen was generated for 3 min with open bottle, followed by 20 min with closed bottle, containing 125 mL CCM. The hydrogen-rich cell culture medium (H-CCM) was sterile filtrated and diluted with normal CCM at dilutions of 1:2 and 1:4 to obtain medium with three different H_2 concentrations.

2.8 Toxicological assays (MTT, BrdU) with test solutions

To investigate the anti-proliferative effect of the prepared test solutions (see 2.7) on human gingival fibroblasts (HGF) a 5-bromo-2'-deoxyuridine (BrdU) assay was performed. The effect on cell viability was investigated with the methyl-thiazolyl-tetrazolium (MTT) assay (both Roche diagnostics, Penzberg). The BrdU assay detects incorporated BrdU into DNA during cell proliferation after addition of substrate labelled antibody (Anti-BrdU), and the MTT assay measures the metabolic activity of the cells by converting the MTT substrate into formazan.

The HGF were seeded in a 96-well plate (4 000 cells/well) and were allowed to adhere for 24 h before incubating with the test solutions for another 24 h. After removing the test solutions, the cells were rinsed with serum-free CCM and fresh medium (100 µL/well) was added. The rinsing step is required to remove magnesium ions, which would interact with the MTT reagent leading to false positive errors.

Then, the BrdU and MTT assay were performed according to the manufacturer's protocol. For the BrdU assay, 10 µL/well BrdU labeling solution was added to the cells (final concentration: 10 µM BrdU/well) and incubated for 4 h under cell culture conditions. After removing the BrdU labeling solution by tapping off, 200 µL/well FixDenat was added for 30 min to fix the cells. FixDenat was removed by tapping and 100 µL/well anti-BrdU-POD working solution was added for 90 min, and then removed by tapping. Cells were rinsed three times with 200 µL/well washing solution and 100 µL/well substrate solution was added. Absorption was measured after 15 min incubation at 370 nm and 492 nm using an ELISA-Reader type infinite M200pro (Tecan Group AG, Männedorf, Switzerland). For the MTT assay, 10 µL/well MTT labeling reagent was added and incubated for 4 h under cell culture conditions. Then, 100 µL/well solubilization solution was added and incubated for 18 h under cell culture condition. Absorption was measured at 555 and 670 nm using the ELISA-Reader. Due to the rapid clearing of hydrogen from the medium, in another well plate, the medium was additionally replaced by fresh H-CCM every 30 min for the first 2.5 h. Then, BrdU and MTT assays were performed. Hence, the cells were affected by a higher hydrogen concentration over a longer period.

2.9 Migration assay with test solutions

The migration assay was performed based on the modified migration assay (Mg-indirect) (see 2.3). Therefore, the labelled HGF were seeded in a 48-well plate to ensure equal cell growth area to the modified migration assay. After scratching and rinsing the confluent cell monolayer, the test solutions were added, and imaging was started. The hydrogen concentration of the various H-CCM and the Mg-extracts were measured up to 60 min in another well-plate, which was placed in the incubator.

2.10 Data and statistical analysis

The measured data were analyzed using descriptive statistics to clarify fundamental effects of the physical cues from the degrading magnesium implants on human cells. Therefore, the data were expressed as the mean ± standard deviation, and the graphics were plotted with Microsoft Excel® software (MS Excel 2016, Washington, USA). To compare the means of two groups, an independent samples t-test was calculated using the Statistical Package for the Social Science (SPSS, v22, Chigago, USA). P-values less than 0.05 were considered statistically significant.

3 Results

3.1 Migration behaviour on Mg, Ti and TCP

The established migration assay allows cell migration studies on pre-corroded magnesium surfaces [4]. To compare the migration behaviour of HGF on magnesium with them on current used membrane materials, the same assay was performed with titanium discs. The results showed that HGF migrate the slowest on pre-corroded magnesium, followed by tissue culture plastic (TCP, control) and the fastest on titanium surfaces (Fig.6). To compare the migration behaviour quantitatively, the value of 50% scratch-area filling of the initial cell-free area was determined for each material. On magnesium, the time $t_{50\%}$ is 22 h, on titanium the $t_{50\%}$ is 8 h and on control surface the $t_{50\%}$ is 13 h.

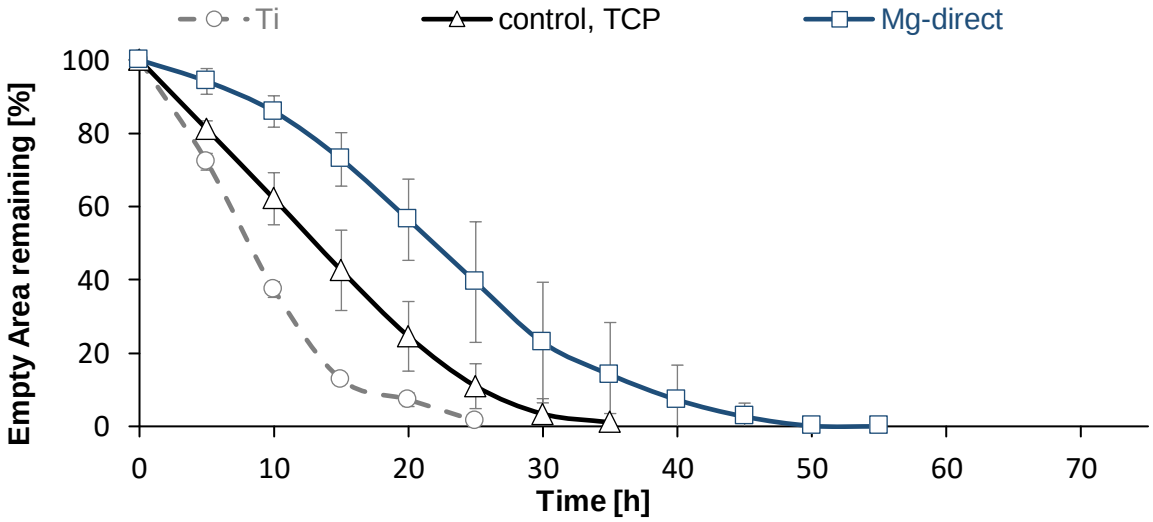

Figure 6. Process of wound closure *in vitro* of HGF on magnesium (Mg-direct), titanium (Ti) and tissue culture plastic (TCP, control) measured on an inverted microscope with a life cell imaging system utilizing the remaining empty scratched area to determine the process of cell migration over time. Data represent the mean±SD (n=4) [4], modified.

3.2 Characterized Mg, Ti and TCP surfaces

To assess the different migration behaviour of HGF on Mg, Ti and TCP, the surfaces of all materials were analyzed. The surface roughness and topography measurements for Mg that were performed during my previous research were completed for Ti and TCP. During corrosion of Mg, the surface becomes obvious with corrosion cracks, which is typical for Mg immersed in physiological solution or cell culture medium [30]. In contrast, the Ti surface exhibits smooth surface with additional parallel microgrooves (Fig.7).

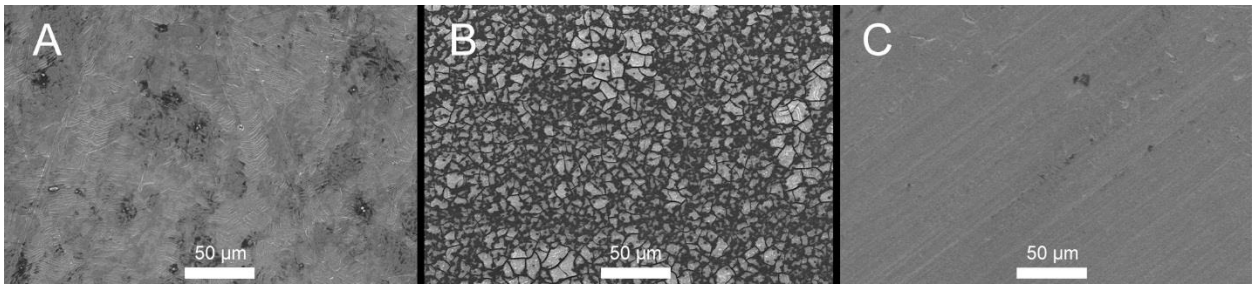

Figure 7. Topography of uncorroded (A), pre-corroded (B) Mg membrane and Ti disc (C) captured with the scanning electron microscopy (SEM), 400x magnification [4].

The roughness of the control surfaces TCP and Ti are significantly smoother compared to magnesium membranes, as the S_a values are much lower, indicated by S_a (Ti) = 74.5 ± 8.7 nm and S_a (TCP) = 10.7 ± 2.4 nm. Pre-corrosion of Mg did not significantly alter the roughness. Pre-corroded Mg has a S_a value of 131.6 ± 4.4 nm, while uncorroded has a S_a value of 129.7 ± 2.2 nm (Fig.8).

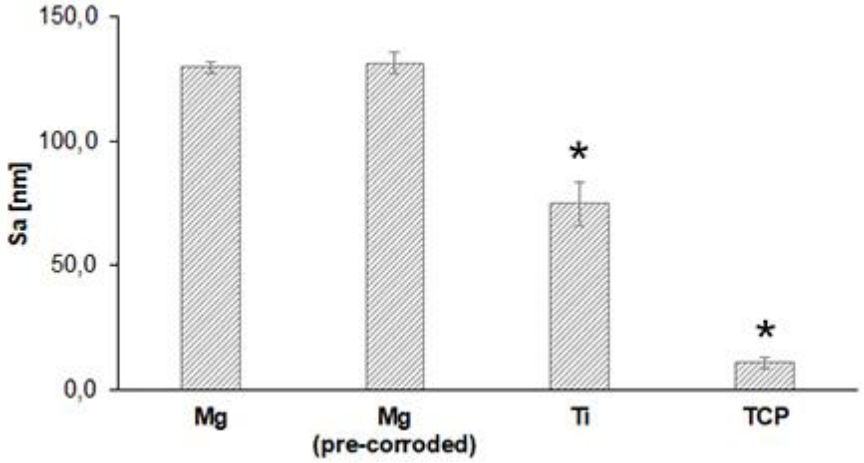

Figure 8. Arithmetic average 3D roughness values (S_a) utilizing atomic force microscopy (AFM) to investigate Mg membranes (uncorroded and pre-corroded), Ti and TCP. Data represent the mean±SD (n=4). Asterisk indicates significant difference ($p<0.05$) to both other test materials [4].

The results of the wettability measurements of Mg, Ti and TCP with the Drop Shape Analyzer are depicted in Figure 9. The water contact angle (WCA) of pre-corroded Mg was the highest (77.8 ± 5.4°), followed by Ti (72.7 ± 7.3°), uncorroded Mg (69.7 ± 2.6°), and the lowest for TCP (48.2 ± 7.9°). Lower WCA values indicate more hydrophilic surfaces, as the surface is readily wettable with water. The surface free energy (SFE) ensues from the WCA and diiodomethane contact angle (DCA). TCP shows the highest SFE (γ = 57.2 ± 7.1 mN m^{-1}), which is in line with the measured hydrophilic WCA value, as surfaces with higher SFE try to lower their energy by adsorbing low energy materials such as hydrocarbon [31].

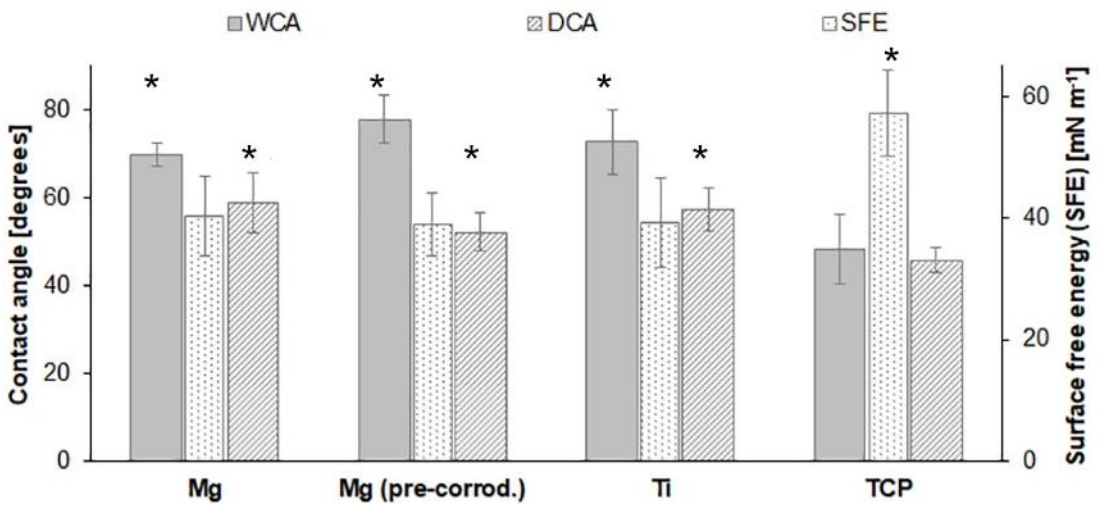

Figure 9. Contact angle for water and diiodomethane of Mg (uncorroded and pre-corroded), Ti and TCP and the resultant surface free energy (SFE). Data represent the mean±SD (n=5). Asterisks represent significant differences compared to the other test materials ($p<0.05$) [4].

3.3 Mg^{2+} affects cell adhesion

The effect of Mg^{2+} on HGF cell adhesion was investigated by immunohistological cell staining of vinculin and actin, including nucleus staining with DAPI after incubation of 24 h with cell culture medium (CCM) containing $MgCl_2 \cdot 6\,H_2O$ (Fig.10). Cells, which were treated with 75 mM $MgCl_2$, showed more green-stained vinculin spots and a more spread cell body compared to cells, treated with 25 mM $MgCl_2$ and the control (treated with CCM). There was no visible difference between the 25 mM $MgCl_2$ and the control cells regarding cell morphology and vinculin amount.

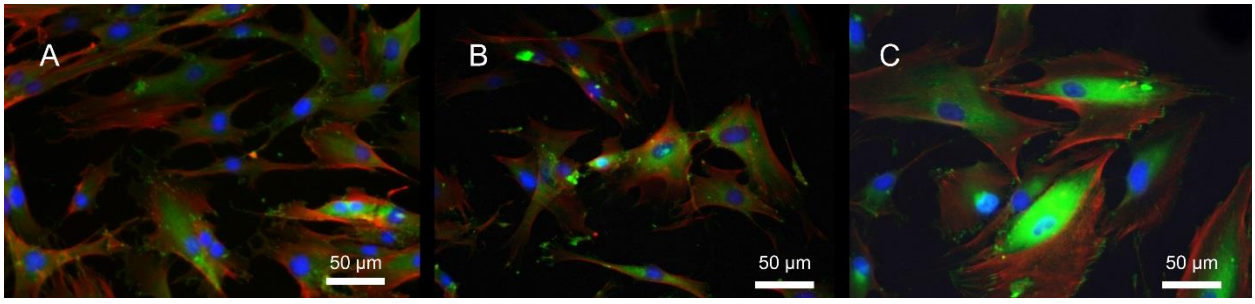

Figure 10. HGF in 80% confluent 48-well plate, treated with cell culture medium (A), containing additionally 25 mM (B) and 75 mM (C) $MgCl_2$ for 24 h and stained for vinculin (green), actin (red) and the nucleus (blue), 40x magnification [4].

3.4 Unmodified vs. modified migration assay (Mg-direct/ Mg-indirect)

The established migration assay (Mg-direct) was modified to exclude the surface effect of corroding magnesium on HGF, ensuring that the cells were only affected by the altered medium (Mg-indirect). The migration curves of both assay variants showed a comparable migration behaviour (Fig.11). With the modified migration assay (Mg-indirect), the time of 50% scratch-area filling of the initial cell-free area was 19 h, while the time was 22 h when HGF migrate directly on the magnesium surface (Mg-direct). The independent samples t-test was performed only for the 20 h time point to compare the migration behaviour between each migration assay (Mg-direct/ Mg-Indirect) and the control in the middle of the migration range.

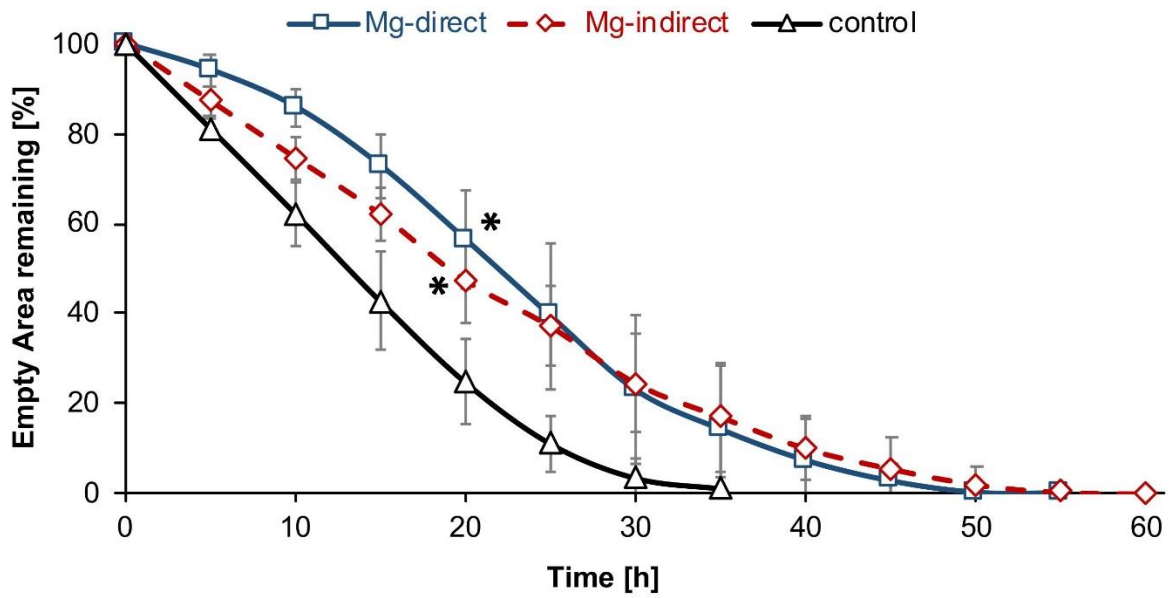

Figure 11. Process of wound closure *in vitro* of HGF on pre-corroded Mg membrane with surface contact (Mg-direct) and without surface contact (Mg-indirect), measured on an inverted microscope with a life cell imaging system utilizing the remaining empty scratched area to determine the process of cell migration over time, control: cell culture medium. Data represent the mean±SD (n=4). Asterisks represent significant differences compared to the control ($p<0.05$) [32].

3.5 Characterized supernatants during cell migration

To confirm the same medium conditions in both migration assays, the supernatants of the HGF were characterized for Mg^{2+}, Ca^{2+} and H_2 concentrations over time. The data for the unmodified (Mg-direct) and modified (Mg-indirect) migration assay, shown in Figure 12, reveal similar trends among each other. The Mg^{2+} concentration increased slightly to 8.5±1.9 mM and the Ca^{2+} concentration decreased slightly over time from 1.17±0.07 mM

to 0.96±0.11 mM. The H_2 concentration was significantly higher than that of the control, indicated by approximately 180±0.20 mM over the entire migration time.

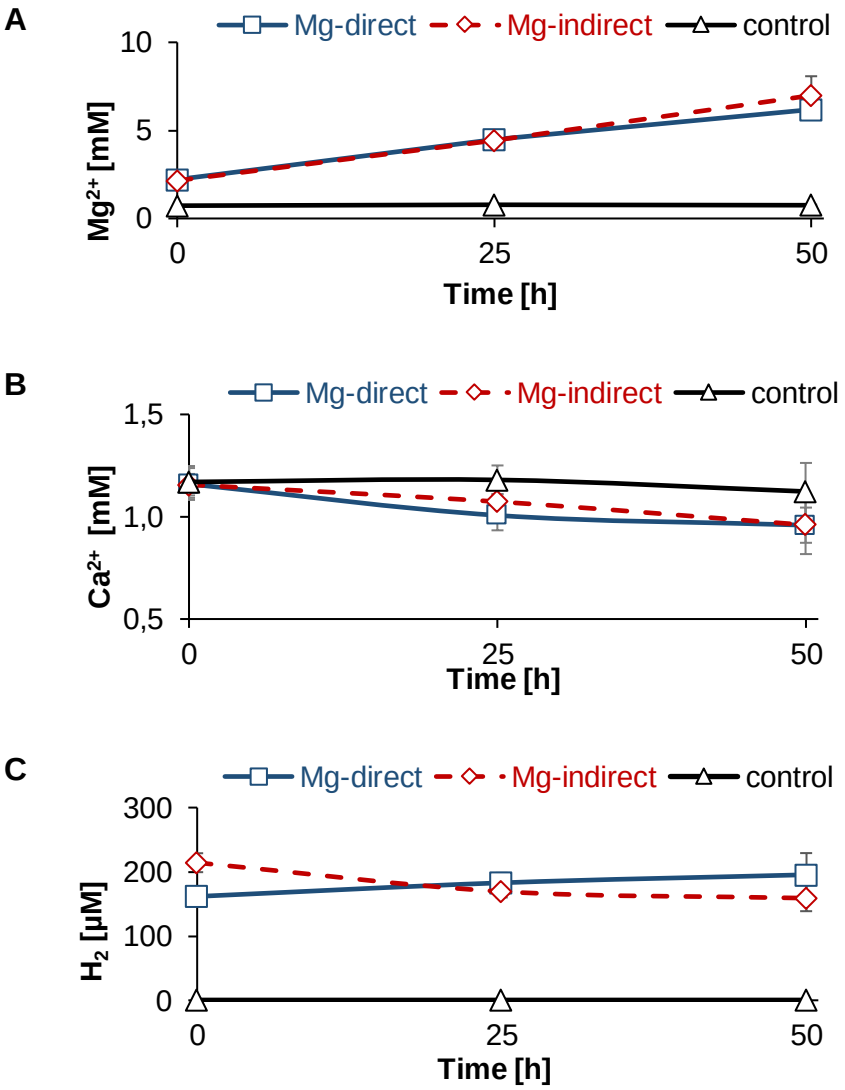

Figure 12. Mg^{2+} (A), Ca^{2+} (B) and H_2 (C) concentrations of the supernatants over time during HGF migration on pre-corroded Mg membrane (Mg-direct) and only affect by corroding Mg membrane in cell culture medium (Mg-indirect), control: cell culture medium. Data represent the mean±SD of three supernatants for each time point (n=3) [32].

3.6 Ca^{2+} storage in the corrosion layer of Mg

The Ca^{2+} analysis of the Mg membranes, obtained from both migration assays (Mg-direct, Mg-indirect) over time, showed an increased amount of Ca^{2+} in the Mg membrane as Ca^{2+} is incorporated in the corrosion layer of Mg (Fig.13). The Ca^{2+} content for the modified migration assay (Mg-direct) showed an increase over time from 1336±63 mg Kg^{-1} to 1931±82 mg Kg^{-1}. During the unmodified migration assay (Mg-indirect) the Ca^{2+} content was almost constant, ranging between 1256±56 and 1361±64 mg Kg^{-1}.

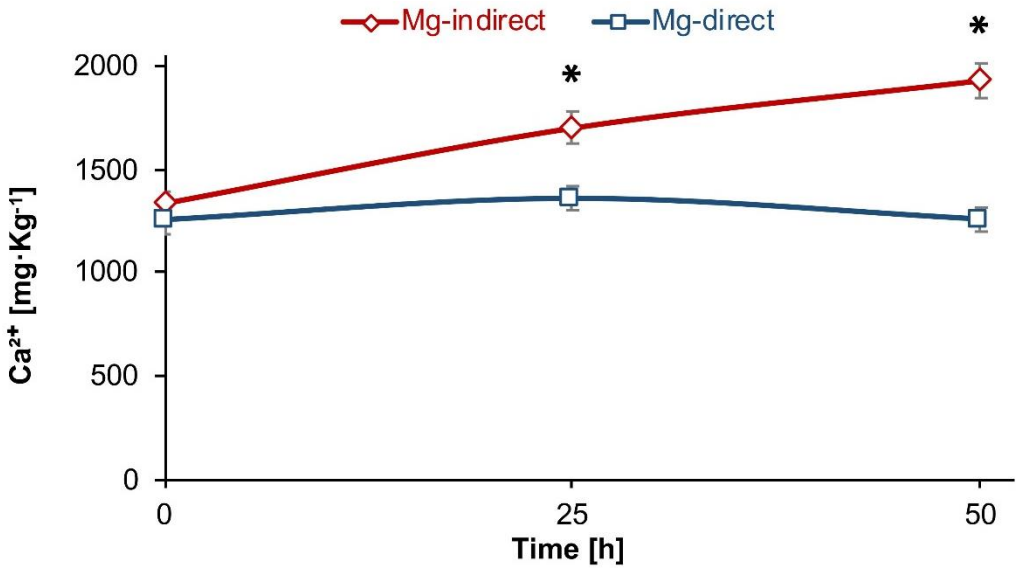

Figure 13. Ca^{2+} concentration of the corrosion layer on pre-corroded Mg membranes during cell migration assay over time with cells directly on Mg (Mg-direct) in comparison to Mg corrosion in a distance to cells (Mg-indirect). Each membrane was measured in triplicate, averaged and indicated as the mean±SD (n=3). Asterisks indicate significant differences between both assays (P<0.05) [32].

3.7 Effect of Mg^{2+} on cells

The effect of Mg^{2+} on cell migration, proliferation and viability of HGF was investigated using a scratch-based migration assay, a BrdU and a MTT assay, while using cell culture medium (CCM) supplemented with $MgCl_2 \cdot 6\ H_2O$. Medium with 25 mM $MgCl_2$ affected neither cell migration nor viability, while at 75 mM $MgCl_2$ the cell migration rate ($t_{50\%}$ = 38 h) was decreased compared to that of the control (CCM, $t_{50\%}$ = 13 h), but the viability was unaltered (Fig.14 A, C). The proliferation rate at 25 mM $MgCl_2$ was slightly increased (124±6) and at 75 mM was greatly decreased (12±7%), compared to that of the control (Fig.14 B).

To consider the increase of osmolality when $MgCl_2$ was added, controls with same osmolality were used, attained by adding mannitol to the CCM. The lower osmolality control (370 mOsmol Kg^{-1}) showed no effect on migration, proliferation and viability (Fig.14). The higher osmolality control (480 mOsmol Kg^{-1}) led to a decreased migration rate ($t_{50\%}$ = 20 h) without affecting cell proliferation and viability.

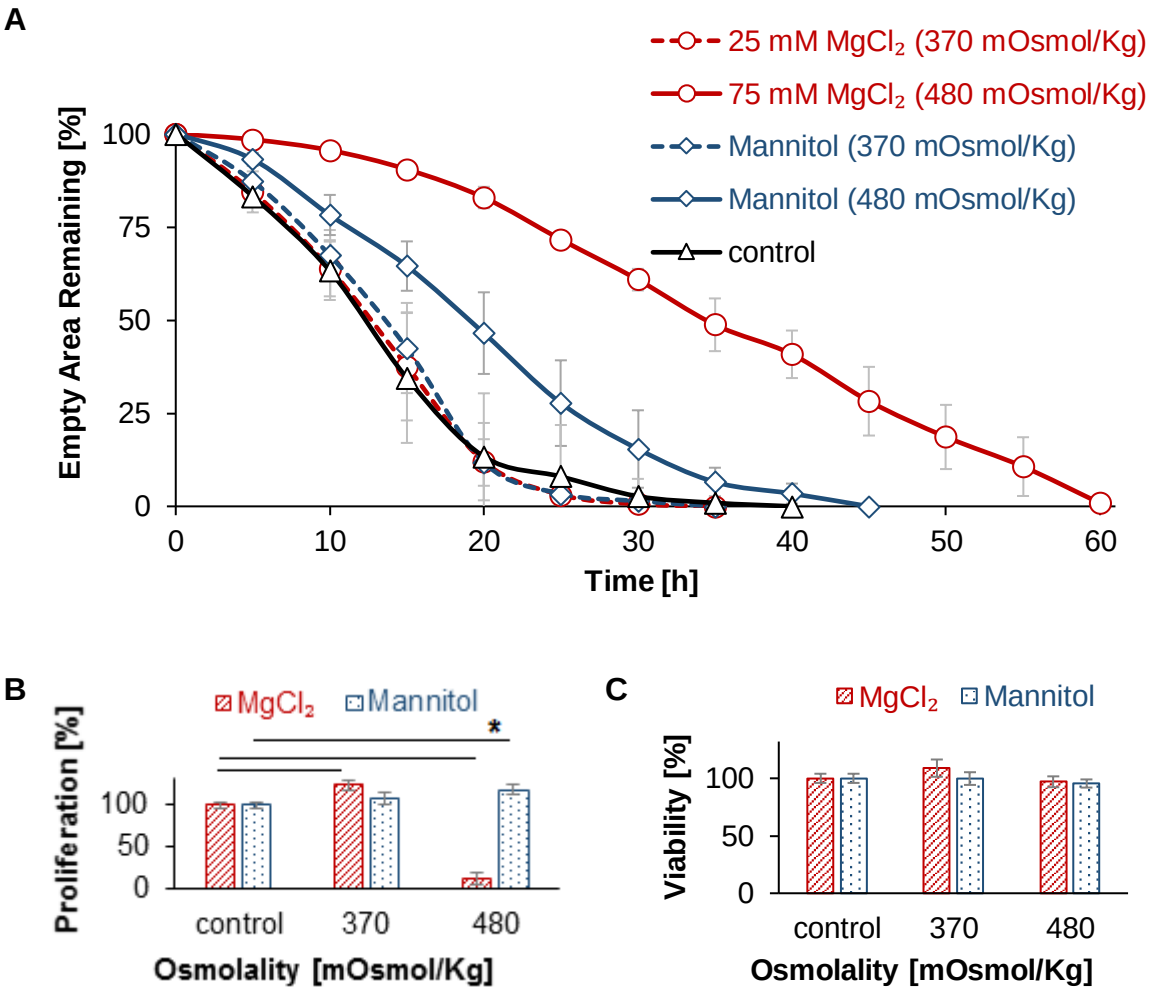

Figure 14. Effect of cell culture medium, supplemented with magnesium chloride ($MgCl_2$), on cell migration (A), proliferation (BrdU assay, B) and viability (MTT assay, C) of HGF, compared to same osmolalities adjusted with mannitol and cell culture medium (control). Test solutions for BrdU and MTT assay were incubated for 24 h, whereas during migration the cells were affected by the test solution until wound closure has been completed. Data represent the mean±SD (migration: n=4; proliferation/viability: n=5). Asterisks indicate significant differences ($P<0.05$) [32].

The increase in Cl^- by adding $MgCl_2$ was considered by using NaCl controls. Cell culture medium (CCM) with 50 mM NaCl has the same Cl^- concentration as CCM with 25 mM $MgCl_2$ and showed only a slight decrease in migration rate compared to 25 mM $MgCl_2$ and the control but did not affect cell proliferation and viability (Fig.15). At 150 mM NaCl, the migration rate was sharply decreased ($t_{50\%}$ = 29 h) compared to the control, but slightly increased compared to CCM with 75 mM $MgCl_2$ ($t_{50\%}$ = 38 h). While at 150 mM NaCl, the viability was not affected, the proliferation rate was sharply reduced in a similar way as the corresponding 75 mM $MgCl_2$ test solution (Fig.15 B, C).

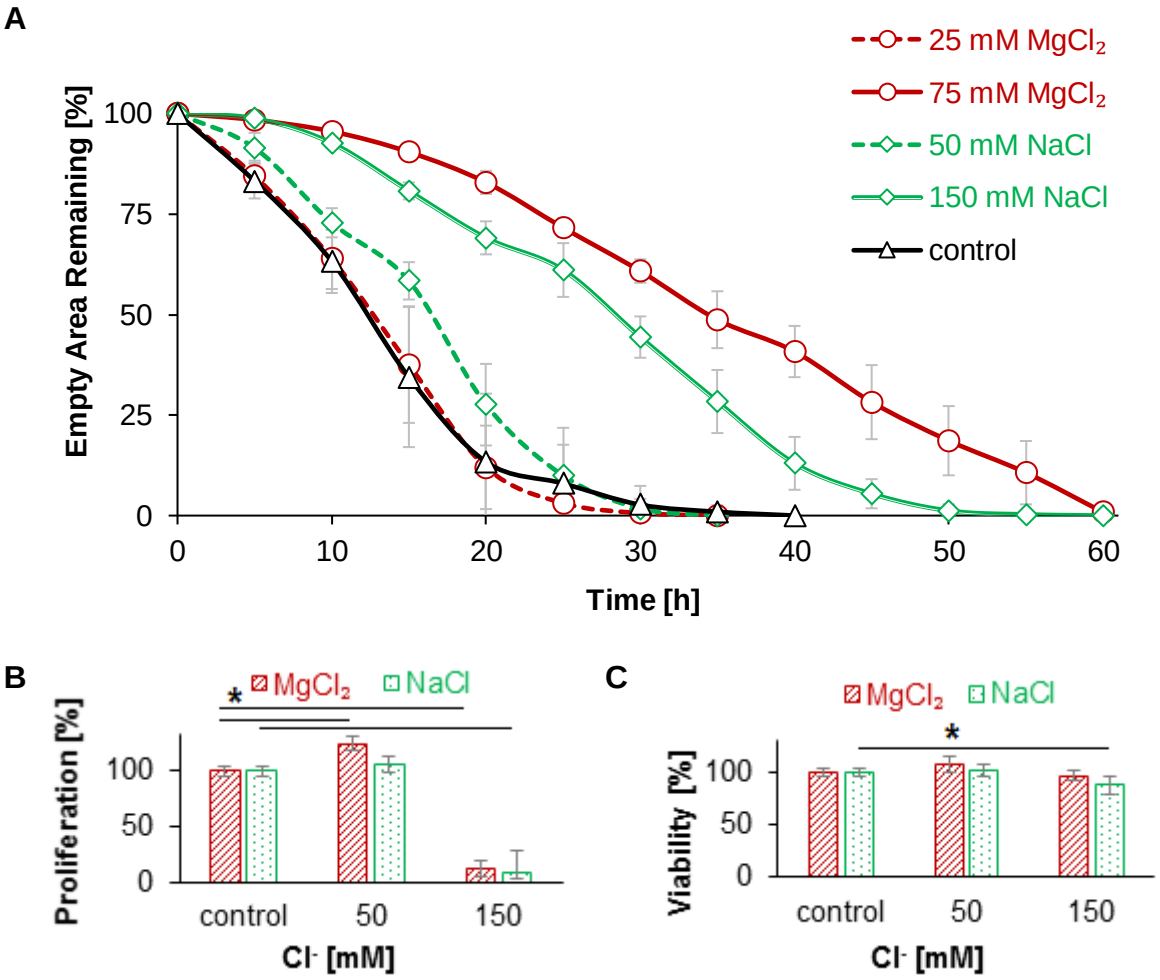

Figure 15. Effect of cell culture medium, supplemented with magnesium chloride ($MgCl_2$), on cell migration (A), proliferation (BrdU assay, B) and viability (MTT assay, C) of HGF, compared to same chloride concentration adjusted with sodium chloride and cell culture medium (control). Test solutions for BrdU and MTT assay were incubated for 24 h, whereas during migration the cells were affected by the test solution until wound closure has been completed. Data represent the mean±SD (migration: n=4; proliferation/viability: n=5). Asterisks indicate significant differences ($P<0.05$) [32].

To exclude the combined effect of osmolality increase and ionic strength increase when $MgCl_2$ was added, further test solutions containing additional mannitol and NaCl were prepared and tested in the assays. The 0 mM, 15 mM and 25 mM $MgCl_2$ test solutions all showed the same osmolality (450±3 mOsmol Kg^{-1}) and ionic strength (75 mM). All test solutions led to slightly slower migration rates compared to the control, but did not differ between each other (Fig.16 A). The cell proliferation and viability were not affected, since at all tested $MgCl_2$ concentrations the percentage values were over 80% compared to the control (Fig.16 B, C).

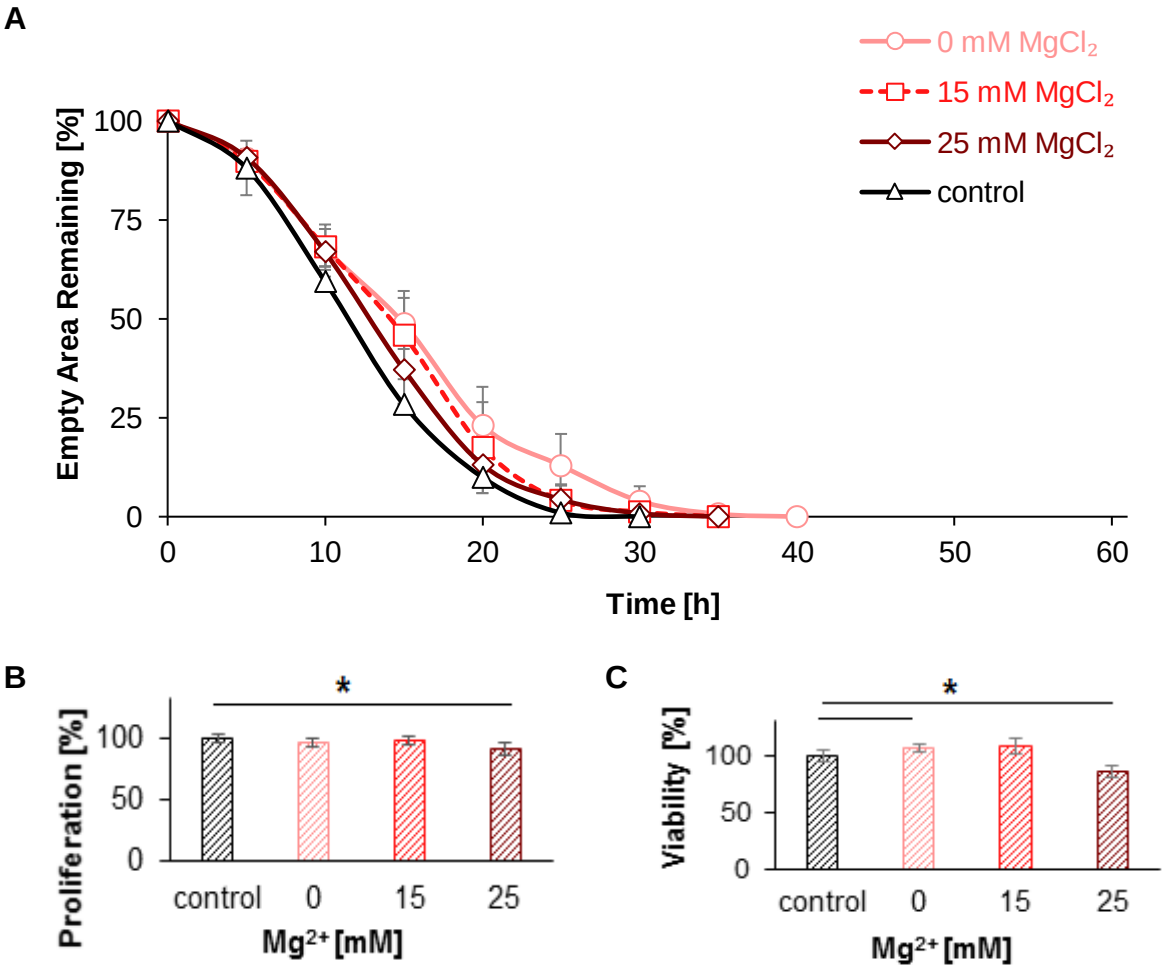

Figure 16. Effect of cell culture medium, supplemented with magnesium chloride ($MgCl_2$), sodium chloride (NaCl) and mannitol to reach the same osmolality (450 mOsmol Kg^{-1}) and ionic strength (75 Mm) on cell migration (A), proliferation (BrdU assay, B) and viability (MTT assay, C) of HGF, compared to cell culture medium (control). Test solutions for BrdU and MTT assay were incubated for 24 h, whereas during migration the cells were affected by the test solution until wound closure has been completed. Data represent the mean±SD (migration: n=4; proliferation/viability: n=6). Asterisks indicate significant differences (P<0.5) [32].

3.8 Effect of Ca^{2+} on cells

Calcium-free cell culture medium was supplemented with $CaCl_2 \cdot 2\ H_2O$ and a migration, BrdU and MTT assays were performed to investigate the cell migration, proliferation and viability of HGF. The migration rate and the proliferation rate decreased with decreasing Ca^{2+} concentration (0.8 mM until 0 mM) (Fig.17 A, B). At 0 mM Ca^{2+} the time to close 50% of the initial cell-free area was 22 h. The control showed the fastest migration rate ($t_{50\%}$ = 13 h) and highest proliferation rate, which represented the highest Ca^{2+} concentration (1.16 mM) compared to the test solutions. All test solutions did not affect viability of HGF, as all percentage values were around 100% (Fig.17 C).

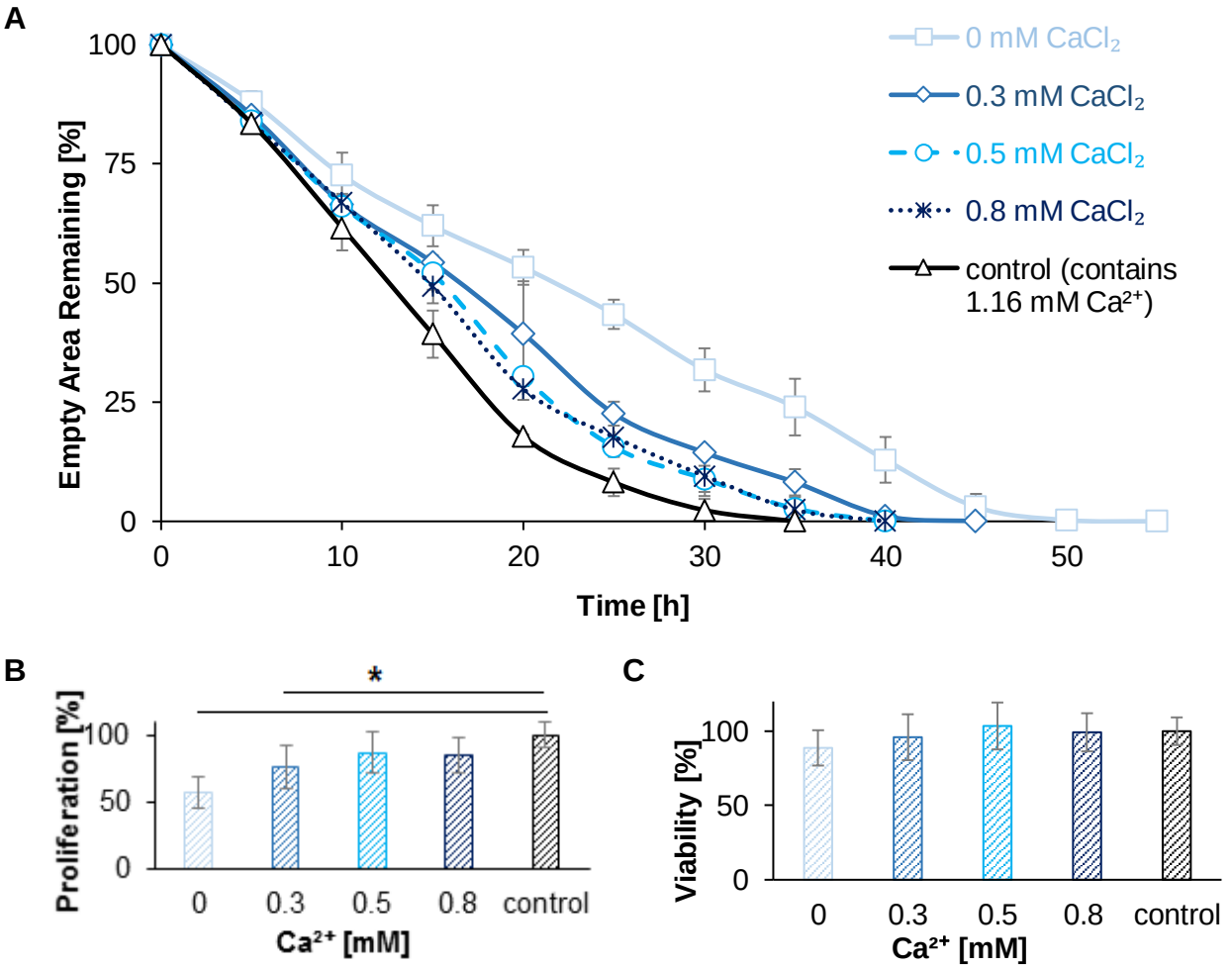

Figure 17. Effect of calcium free cell culture medium, supplemented with calcium chloride ($CaCl_2$) on cell migration (A), proliferation (BrdU assay, B) and viability (MTT assay, C) of HGF, compared to cell culture medium (control). Test solutions for BrdU and MTT assay were incubated for 24 h, whereas during migration the cells were affected by the test solution until wound closure has been completed. Data represent the mean±SD (migration: n=4; proliferation/viability: n=6). Asterisks indicate significant differences (P<0.5) [32].

3.9 Effect of H_2 on cells

Cell culture medium was enriched with H_2 (H-CCM) and two dilutions were prepared, which were all tested in the migration, BrdU and MTT assays to investigate cell migration, proliferation and viability of HGF. Neither the undiluted nor the diluted H-CCM affected migration rate, as well as proliferation and viability (Fig.18 A, C, D). The initial H_2 concentration of undiluted (337±53 µM) and diluted H-CCM (123±6 µM and 46±3 µM) decreased over time and was no longer detectable after 60 min (Fig.18 B). Replacing the H-CCM every 30 min for the first 2.5 h affected neither proliferation nor viability of HGF (Fig.19).

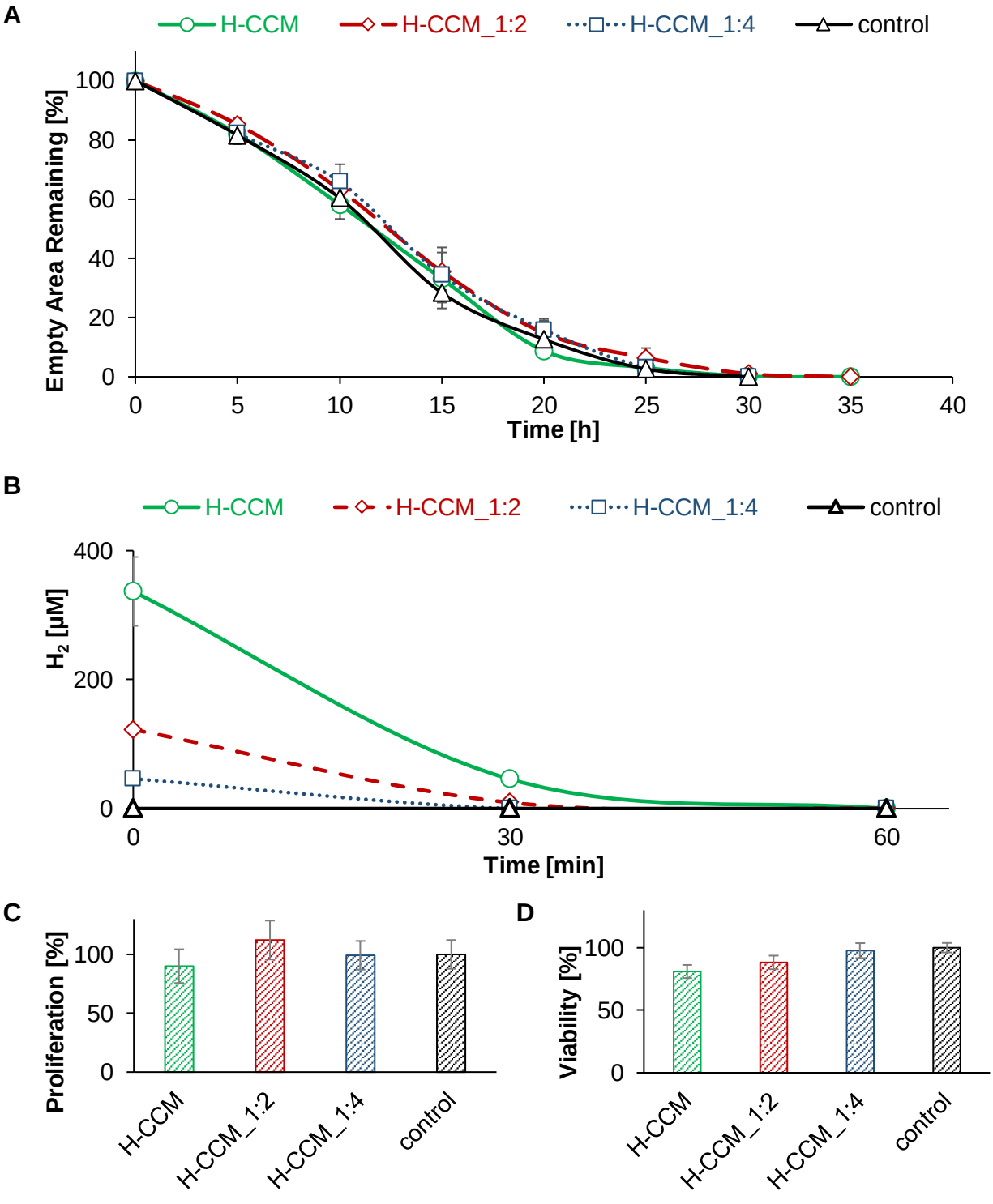

Figure 18. Effect of hydrogen-rich cell culture medium (H-CCM), generated with the Highdrogen Age2 Go for 23 min and two dilutions with CCM (1:2 and 1:4) on cell migration (A), proliferation (BrdU assay, C) and viability (MTT assay, D) of HGF compared to control (CCM). H-CCM for BrdU and MTT assay were incubated for 24 h, whereas during migration the cells were affected by H-CCM until wound closure has been completed. Data represent the mean±SD (migration: n=4; proliferation/viability: n=8). The H_2 concentration was measured for 30s at 0 h, after 0.5 h and after 1 h (C) during incubation under cell culture conditions and averaged (n=3). There is no significant difference between the H-CCM solutions and the control from the proliferation and viability assays. [32].

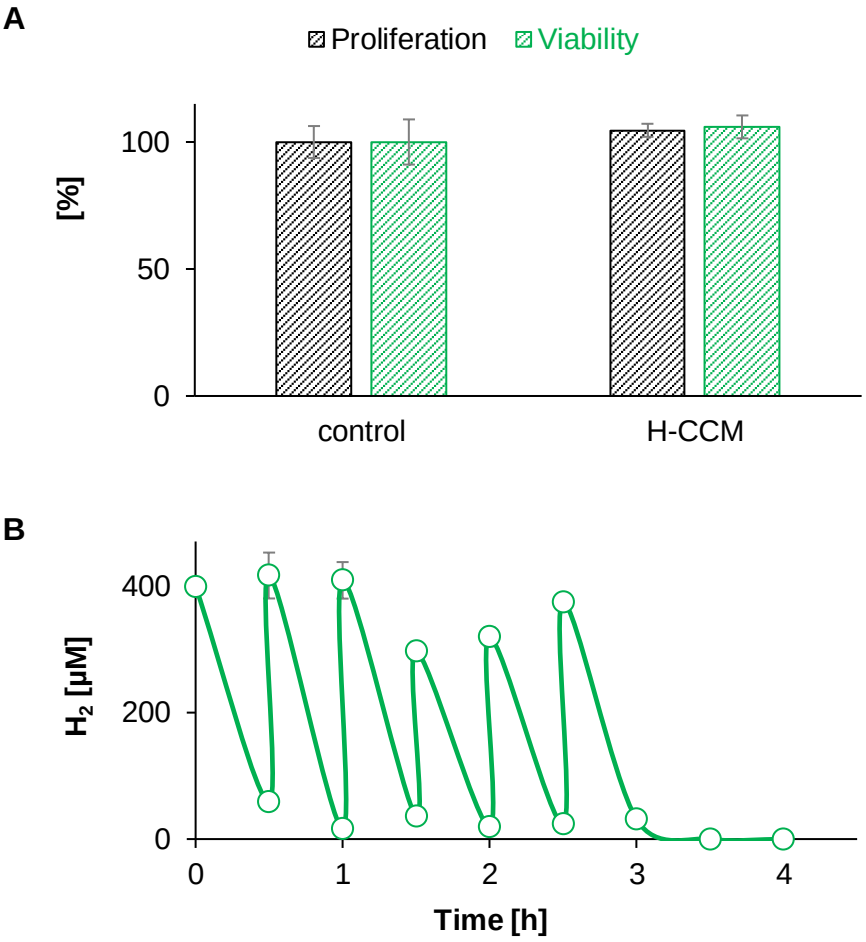

Figure 19. Effect of hydrogen-rich cell culture medium (H-CCM), generated with the Highdrogen Age$_2$ Go for 23 min, on cell proliferation (BrdU assay) and viability (MTT assay) of HGF compared to control (CCM) (A). H-CCM was renewed every 30 min over the first 2.5 h of the whole 24 h incubation time. Data represent the mean±SD (n=6). The H_2 concentration was measured for 30s (C) during incubation under cell culture conditions and averaged (n=3). There is no significant difference between the H-CCM and the control from the proliferation and viability assays [32].

3.10 Effect of Mg extracts on cells

The combined effect of all altered medium-related physical cues of corroding magnesium on HGF were analyzed by testing Mg extracts regarding cell migration, proliferation and viability. The Mg extracts were obtained by immersing the magnesium membrane in cell culture medium (CCM) with (w CO_2) and without (w/o CO_2) carbon dioxide exchange. Incubation with Mg-extract (w/o CO_2) led to a slightly slower migration rate ($t_{50\%}$ = 15 h) compared to the control (Fig.20 A), without affecting cell proliferation and viability (Fig.20 B, C). In contrast, when cells were incubated with Mg-extract (w CO_2), no migration rate was detectable as the cells became rounded after 5 h and remained in their position over the whole assay time. Additionally, the proliferation and viability were below 75% compared to the control.

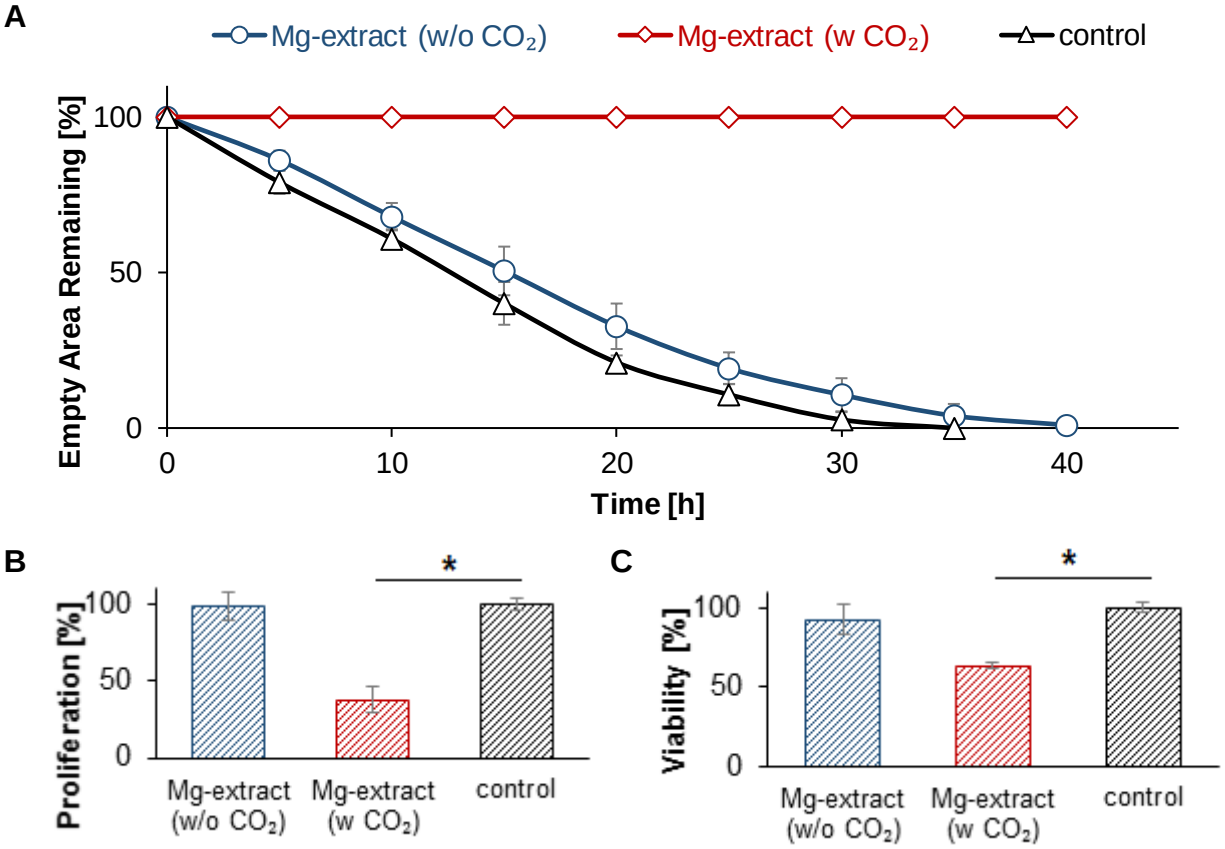

Figure 20. Effect of Mg extracts, received by corrosion of the Mg membrane (10x10mm), 140 µm thickness) in 10 mL cell culture medium with and without CO_2 exchange (w CO_2) and without (w/o CO_2) on cell migration (A), proliferation (B) and viability (C) of HGF. Mg extracts for BrdU and MTT assay were incubated for 24 h, whereas during migration the cells were affected by Mg extracts until wound closure has been completed. Data represent the mean±SD (migration: n=4; proliferation/viability: n=4). Asterisks indicates significant differences ($P<0.05$) [32].

The measured H_2, Mg^{2+} and Ca^{2+} concentrations of both Mg extracts over time are presented in Figure 21. The H_2 concentration of both extracts was, negligibly small, with values below 4 µm directly after preparing the extracts and was not detectable anymore after 15 min. The Mg-extract (w CO_2) revealed an extremely elevated Mg^{2+} concentration (58±1 mM) and a reduced Ca^{2+} concentration (0.57±0.01 mM) compared to the Mg-extract (w/o CO_2) and to the control. The Mg^{2+} concentration of the Mg-extract (w/o CO_2) was 4.4±0.01 mM and the Ca^{2+} concentration was 0.93±0.02 mM.

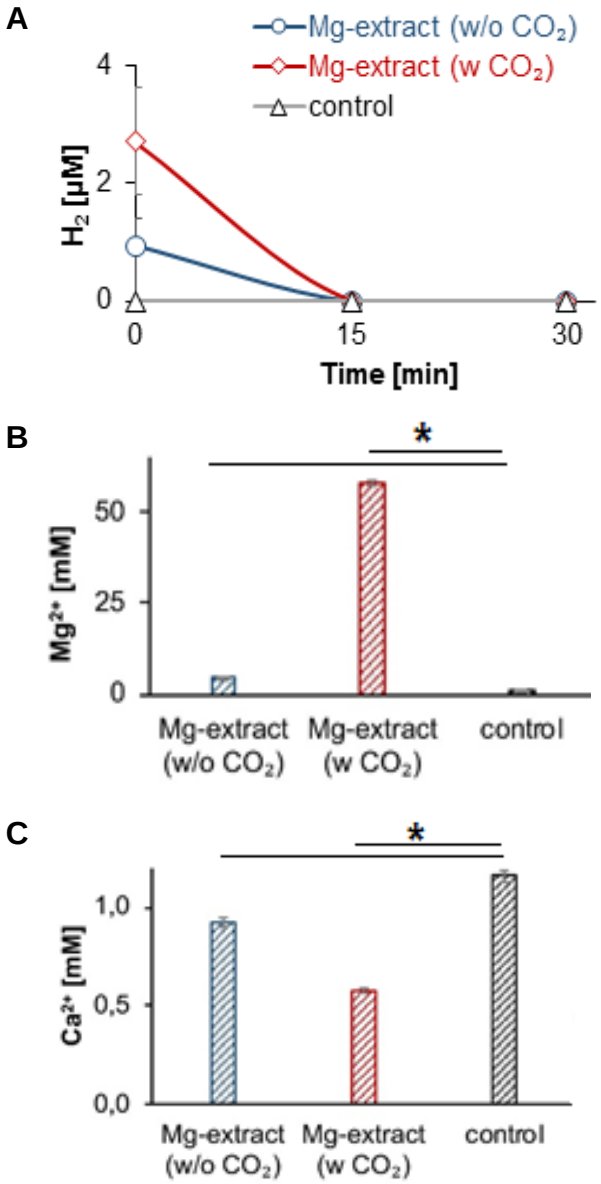

Figure 21. The H_2 (A), Mg^{2+} (B) and Ca^{2+} (C) concentration of the Mg-extracts (w/o CO_2, w CO_2), which were tested in the migration, proliferation and viability assay. The Mg^{2+} and Ca^{2+} concentrations were measured in triplicate of each extract, averaged and indicated as the mean±SD of three independent prepared extracts (n=3). The H_2 concentration was measured for 30 s, averaged and indicated as the mean±SD of three independent prepared extracts (n=3). Asterisks indicate significant differences ($P<0.05$) [32].

4 Discussion

Magnesium-based implants are very promising in application for dentistry, due to their excellent biocompatibility and biodegradability. Thus, barrier membranes made of pure magnesium can be used for Guided Bone Regeneration (GBR) procedures [1, 4]. Due to the often reported membrane exposure associated with utilized non-resorbable membrane materials made of titanium, cell migration of human gingival fibroblasts (HGF) on the barrier membrane is crucial to close the exposed membrane and to ensure optimal healing success [8]. Cell migration of HGF on magnesium membranes was already investigated *in vitro* and *in vivo* during my previous research [4]. However, there is no comparison to membrane materials that are currently used. Regarding cell migration studies on magnesium surfaces, we must consider that magnesium degrades by forming magnesium ions, molecular hydrogen and hydroxide ions [1]. Furthermore, the surface is altered due to formation of a corrosion layer [12]. All parameters affecting cell behaviour, including cell migration, viability and proliferation are called 'physical cues'. The effect of physical cues on cell behaviour of HGF has not been investigated in detail. Identification of possible effects, especially on HGF migration, including specific concentration of the medium-altered physical cues, will provide knowledge to design the targeted magnesium corrosion rate for optimal healing success.

In this study, the migration behaviour of HGF on titanium surfaces was analyzed, including surface measurements to characterize the surface wettability, roughness and topography, and to compare these results with existing results for magnesium. To prove our assumption that medium alterations caused by magnesium corrosion have a major impact on cell migration rather than surface alterations, the migration assay was modified to exclude the surface impact. As a main part of this study, the effect of the different medium-altered physical cues on cell migration, proliferation and viability of the HGF was analyzed to explain the migration behaviour on magnesium membranes. Our results showed that cell migration on magnesium surfaces is 1.7 fold slower compared to tissue culture plastic and 2.8 fold slower compared to titanium. We demonstrated that migration rate is mainly affected by medium alterations, while the surface has only a minor effect, verified by performing the modified migration assay. More specifically, we identified the Mg^{2+}/Ca^{2+} ratio and the constantly elevated H_2 level as parameters that seem to explain the slow migration behaviour of HGF on magnesium membranes.

Surface measurements yielded roughness values below 200 nm for magnesium (pre-corroded/ uncorroded), titanium and tissue culture plastic. We did not find a correlation between migration rate and roughness. According a study of Kim *et al*. [33] roughness has no influence on cell attachment of HGF in the range of 200 nm or less. Accordingly, HGF attachment is mainly affected by hydrophilicity with highest fibroblast adhesion and proliferation at a water contact angle (WCA) between 50° and 60° [34]. As already known, high cell attachment leads to a slower migration rate [35]. The comparison to the control surfaces shows that cell migration is faster on titanium than on tissue culture plastic surfaces. This can be explained by the lower hydrophilicity of the tissue culture plastic surface, which is in the stated range for highest fibroblast attachment and slower cell migration. Magnesium showed almost the same WCA as titanium, but the HGF migration was significantly reduced. Therefore, we assumed that the surface condition of magnesium does not determine cell migration on magnesium membranes.

Immunohistological investigations of cellular structure showed that HGF treated with medium containing 75 mM $MgCl_2$ lead to increased focal adhesions, showing that the Mg^{2+} concentration is one physical cue that affects cell adhesion as a crucial parameter for cell migration. The modified migration assay allowed to exclude all surface impacts to ensure that the cells were only affected by the dissolved corrosion products of magnesium. Our results showed that cell migration of each assay (modified/unmodified) is comparable. Therefore, we demonstrated that medium alterations caused by magnesium corrosion are the main reason for slower migration rate on magnesium membranes. Moreover, the characterized supernatants over time during cell migration showed similar Mg^{2+}, Ca^{2+} and H_2 concentrations for both assays.

To obtain more precise results of how each medium-altered physical cue affects cell migration, cell culture medium supplemented with Mg and Ca salts, as well as H_2 enriched medium was tested. Moreover, the combined effect of single physical cues was investigated by preparing different magnesium extracts.

Cell culture medium supplemented with magnesium chloride showed no effects on HGF migration, proliferation or viability up to 25 mM. The cell migration and proliferation were sharply reduced only at 75 mM. We could exclude effects of increasing osmolality and chloride concentrations when magnesium chloride was added by using adequate controls. By comparing this result with the determined Mg^{2+} concentration during the cell migration assay on magnesium membranes we could exclude the Mg^{2+} concentration as a single potential physical cue affecting migration rate, since the Mg^{2+} concentration

during the migration assay was below 25 mM. We only measured the concentration of the whole supernatant; therefore, we cannot exclude the possibility that the Mg^{2+} concentration directly on the Mg surface may have been slightly higher.

Increasing the calcium chloride concentration from 0 mM to 0.8 mM in the medium by using calcium-free cell culture medium lead to an increased migration rate. These results are in line with the literature as Ca^{2+} is required for cell detachment resulting in faster cell migration [36, 37]. During HGF migration on Mg surfaces, the Ca^{2+} concentration of the supernatant decreased only slightly from 1.16 mM to 0.95 mM. The Ca^{2+} decrease can be explained by $Ca_5(PO_4)(OH)$ and $Ca_3(PO_4)_2$ precipitation in the corrosion layer [38], which could be confirmed by ICP-OES in our studies. Combining both results, we assume, that the slightly Ca^{2+} decrease during cell migration on Mg surfaces only makes a very small contribution to the slow migration rate of HGF.

Furthermore, the effect of H_2 enriched cell culture medium on cell behaviour of HGF was tested. Our results showed that initial concentrations up to 336 µM had no effect on cell migration, proliferation and viability. Due to the rapid clearing, the H_2 of the medium was completely eliminated after 60 min. Therefore, we could not ensure conditions identical to our established migration assay on magnesium surfaces having constant H_2 concentration of 180 µM over 50 h. According to the literature HGF even react after short exposure of 2 h to H_2 enriched cell culture medium (690 µM) as cell migration and proliferation was promoted resulting in faster wound healing *in vitro* [39]. Therefore, we assumed that HGF only react at higher H_2 concentration.

Finally, we tested two different prepared magnesium extracts (with and without CO_2) to investigate the combined effect of all medium-altered physical cues on HGF migration. Both prepared Mg extracts showed negligibly small initial H_2 concentrations of 4 µM.

Magnesium extract without CO_2 exchange lead to a slightly reduced cell migration rate, although the Mg^{2+} concentration was only slightly increased (4.5 mM) and the Ca^{2+} concentration slightly decreased (0.93 mM). As we cannot explain the reduced migration rate with the slightly increased Mg^{2+} concentration, we can conclude that the decrease of Ca^{2+} might affect migration rate. The effect becomes more obvious at tested Mg extract with CO_2, as there was no cell migration detectable, although the Mg^{2+} concentration was below 75 mM. In this concentration range, cell migration might be possible even in a reduced way.

These results revealed that it is not the absolute concentration of both ions that determines migration behaviour, but that the ratio between Mg^{2+} and Ca^{2+} is more crucial,

which can be supported by literature [36, 37, 40]. The Mg^{2+}/Ca^{2+} ratio of the Mg extract with CO_2 exchange was 102 and without CO_2 exchange was 5 (for comparison: control = 0.6).

By applying this knowledge to the established migration assay on magnesium, we showed an increase in the Mg^{2+}/Ca^{2+} ratio from 1.8 at the beginning to 4.4 after 25 h and to 7.4 after 50 h. Interestingly, the ratio after 25 h was almost the same as the ratio of the Mg extract without CO_2. However, the migration rate on Mg membranes is slower compared to the Mg extract without CO_2. The only difference is that, during migration on Mg membranes, the H_2 concentration is constantly 180 µM; during migration incubating with Mg extract without CO_2, the H_2 concentration remained at zero after 15 min for the whole migration assay period. Therefore, we assume, that not only the Mg^{2+}/Ca^{2+} ratio affects migration behaviour but that the combination of Mg^{2+}/Ca^{2+} ratio and dissolved H_2 in the cell culture medium lead to reduced migration rate on Mg surfaces. This study provides primary results of migration studies of HGF on Mg membranes, which should resemble the migration behaviour of HGF during the initial hours of Mg implantation *in vivo*. However, this study has potential limitations. In order to get more reliable results the analysis should be performed with more replicates. Furthermore, the applicability of *in vitro* experiments to *in vivo* situations is very debatably, as the *in vitro* conditions can not completely simulate the *in vivo* situations. However, with the knowledge of this study the environmental conditions during the application of Mg membranes in GBR procedure can be changed in order to ensure faster wound healing.

5 Literature

[1] Zhao D, Witte F, Lu F, Wang J, Li J, Qin L. Current status on clinical applications of magnesium-based orthopaedic implants: A review from clinical translational perspective. Biomaterials 2017;112:287-302.
[2] Sissi C, Palumbo M. Effects of magnesium and related divalent metal ions in topoisomerase structure and function. Nucleic Acids Research 2009;37:702-11.
[3] Waizy H, Seitz J-M, Reifenrath J, Weizbauer A, Bach F-W, Meyer-Lindenberg A, Denkena B, Windhagen H. Biodegradable magnesium implants for orthopedic applications. Journal of Materials Science 2013;48:39-50.
[4] Amberg R, Elad A, Rothamel D, Fienitz T, Szakacs G, Heilmann S, Witte F. Design of a migration assay for human gingival fibroblasts on biodegradable magnesium surfaces. Acta Biomaterialia 2018.
[5] Liu J, Kerns DG. Mechanisms of Guided Bone Regeneration: A Review. The Open Dentistry Journal 2014;8:56-65.
[6] Robinson DA, Griffith RW, Shechtman D, Evans RB, Conzemius MG. In vitro antibacterial properties of magnesium metal against Escherichia coli, Pseudomonas aeruginosa and Staphylococcus aureus. Acta Biomater 2010;6:1869-77.
[7] Burmester A, Willumeit-Romer R, Feyerabend F. Behavior of bone cells in contact with magnesium implant material. J Biomed Mater Res B Appl Biomater 2017;105:165-79.
[8] Zitzmann N, Naef R, Schärer P. Resorbable Versus Nonresorbable Membranes in Combination with Bio-Oss for Guided Bone Regeneration1997.
[9] Lang NP, Hämmerle CHF, Brägger U, Lehmann B, Nyman SR. Guided tissue regeneration in jawbone defects prior to implant placement. Clinical Oral Implants Research 1994;5:92-7.
[10] Behring J, Junker R, Walboomers XF, Chessnut B, Jansen JA. Toward guided tissue and bone regeneration: morphology, attachment, proliferation, and migration of cells cultured on collagen barrier membranes. A systematic review. Odontology 2008;96:1-11.
[11] Li L, Zhang M, Li Y, Zhao J, Qin L, Lai Y. Corrosion and biocompatibility improvement of magnesium-based alloys as bone implant materials: a review. Regenerative Biomaterials 2017.
[12] Charyeva O, Feyerabend F, Willumeit R, Zukowski D, Gasqueres C, Szakács G, Ahmad Agha N, Hort N, Gensch F, Cecchinato F, Jimbo R, Wennerberg A, Lips K. In Vitro Resorption of Magnesium Materials and its Effect on Surface and Surrounding Environment2015.
[13] Günzler H, Bahadir AM, Danzer K, Engewald W, Fresenius W, Galensa R, Huber W, Linscheid M, Schwedt G, Tölg G. Analytiker-Taschenbuch: Springer Berlin Heidelberg; 2013.
[14] Ul-Hamid A. A Beginners' Guide to Scanning Electron Microscopy: Springer International Publishing; 2018.
[15] Michler GH. Electron Microscopy of Polymers: Springer Berlin Heidelberg; 2008.
[16] Emter E. Literatur und Quantentheorie: die Rezeption der modernen Physik in Schriften zur Literatur und Philosophie deutschprachiger Autoren (1925-1970): De Gruyter; 1995.
[17] Schatten H. Scanning Electron Microscopy for the Life Sciences: Cambridge University Press; 2013.
[18] Flegler SL, Heckman JW, Klomparens KL. Elektronenmikroskopie: Grundladen-Methoden-Anwendungen. Heidelberg: Spektrum Akademischer Verlag; 1995.
[19] Braga PC, Ricci D. Atomic Force Microscopy: Biomedical Methods and Applications: Humana Press; 2004.
[20] Halevi G. Process and Operation Planning: Revised Edition of The Principles of Process Planning: A Logical Approach: Springer Netherlands; 2003.
[21] Haas W. Oberflächenbeurteilung- Rauheitsmessung. In: Universität, editor. Stuttgart2012. p. 1-18.

[22] Stout KJ. Development of Methods for the Characterisation of Roughness in Three Dimensions: Penton Press; 2000.
[23] Bellitto V. Atomic Force Microscopy: Imaging, Measuring and Manipulating Surfaces at the Atomic Scale: IntechOpen; 2012.
[24] Voigtländer B. Scanning Probe Microscopy: Atomic Force Microscopy and Scanning Tunneling Microscopy: Springer Berlin Heidelberg; 2015.
[25] Morita S, Giessibl FJ, Wiesendanger R. Noncontact Atomic Force Microscopy: Springer Berlin Heidelberg; 2009.
[26] Eaton P, West P. Atomic Force Microscopy: OUP Oxford; 2010.
[27] Berg J. Wettability: CRC Press; 1993.
[28] Owens DK, Wendt RC. Estimation of the surface free energy of polymers. Journal of Applied Polymer Science 1969;13:1741-7.
[29] Kaelble D. Dispersion-polar surface tension properties of organic solids. The Journal of Adhesion 1970;2:66-81.
[30] Pan C-J, Pang L-Q, Hou Y, Lin Y-B, Gong T, Liu T, Ye W, Ding H-Y. Improving Corrosion Resistance and Biocompatibility of Magnesium Alloy by Sodium Hydroxide and Hydrofluoric Acid Treatments. Applied Sciences 2016;7:33.
[31] Mattox DM. Chapter 2 - Substrate ("Real") Surfaces and Surface Modification. In: Mattox DM, editor. Handbook of Physical Vapor Deposition (PVD) Processing (Second Edition). Boston: William Andrew Publishing; 2010. p. 25-72.
[32] Amberg R, Elad A, Beuer F, Vogt C, Bode J, Witte F. Effect of physical cues of altered extract media from biodegradable magnesium implants on human gingival fibroblasts. Acta Biomaterialia 2019.
[33] Kim YS, Shin SY, Moon SK, Yang SM. Surface properties correlated with the human gingival fibroblasts attachment on various materials for implant abutments: a multiple regression analysis. Acta odontologica Scandinavica 2015;73:38-47.
[34] Kim SH, Ha HJ, Ko YK, Yoon SJ, Rhee JM, Kim MS, Lee HB, Khang G. Correlation of proliferation, morphology and biological responses of fibroblasts on LDPE with different surface wettability. J Biomater Sci Polym Ed 2007;18:609-22.
[35] DiMilla PA, Barbee K, Lauffenburger DA. Mathematical model for the effects of adhesion and mechanics on cell migration speed. Biophysical Journal 1991;60:15-37.
[36] Lange TS, Bielinsky AK, Kirchberg K, Bank I, Herrmann K, Krieg T, Scharffetter-Kochanek K. Mg2+ and Ca2+ Differentially Regulate β1 Integrin-Mediated Adhesion of Dermal Fibroblasts and Keratinocytes to Various Extracellular Matrix Proteins. Experimental Cell Research 1994;214:381-8.
[37] Lange TS, Kirchberg K, Bielinsky AK, Leuker A, Bank I, Ruzicka T, Scharffetter-Kochanek K. Divalent cations (Mg2+, Ca2+) differentially influence the β1 integrin-mediated migration of human fibroblasts and keratinocytes to different extracellular matrix proteins. Experimental dermatology 1995;4:130-7.
[38] Willumeit R, Fischer J, Feyerabend F, Hort N, Bismayer U, Heidrich S, Mihailova B. Chemical surface alteration of biodegradable magnesium exposed to corrosion media. Acta Biomater 2011;7:2704-15.
[39] Xiao L, Miwa N. Hydrogen-rich water achieves cytoprotection from oxidative stress injury in human gingival fibroblasts in culture or 3D-tissue equivalents, and wound-healing promotion, together with ROS-scavenging and relief from glutathione diminishment. Human Cell 2017;30:72-87.
[40] Grzesiak JJ, Pierschbacher MD. Shifts in the concentrations of magnesium and calcium in early porcine and rat wound fluids activate the cell migratory response. The Journal of clinical investigation 1995;95:227-33.

Eidesstattliche Versicherung

„Ich, Romina Amberg, versichere an Eides statt durch meine eigenhändige Unterschrift, dass ich die vorgelegte Dissertation mit dem Thema: „Influence of physical cues from the degrading magnesium implants on human cells“ (dt.: Einfluss der *Physical Cues* der degradierenden Magnesiumimplantate auf humane Zellen) selbstständig und ohne nicht offengelegte Hilfe Dritter verfasst und keine anderen als die angegebenen Quellen und Hilfsmittel genutzt habe.
Alle Stellen, die wörtlich oder dem Sinne nach auf Publikationen oder Vorträgen anderer Autoren beruhen, sind als solche in korrekter Zitierung kenntlich gemacht. Die Abschnitte zu Methodik (insbesondere praktische Arbeiten, Laborbestimmungen, statistische Aufarbeitung) und Resultaten (insbesondere Abbildungen, Graphiken und Tabellen werden von mir verantwortet.

Meine Anteile an etwaigen Publikationen zu dieser Dissertation entsprechen denen, die in der untenstehenden gemeinsamen Erklärung mit dem Betreuer, angegeben sind. Für sämtliche im Rahmen der Dissertation entstandenen Publikationen wurden die Richtlinien des ICMJE (International Committee of Medical Journal Editors; www.icmje.og) zur Autorenschaft eingehalten. Ich erkläre ferner, dass mir die Satzung der Charité – Universitätsmedizin Berlin zur Sicherung Guter Wissenschaftlicher Praxis bekannt ist und ich mich zur Einhaltung dieser Satzung verpflichte.

Die Bedeutung dieser eidesstattlichen Versicherung und die strafrechtlichen Folgen einer unwahren eidesstattlichen Versicherung (§156,161 des Strafgesetzbuches) sind mir bekannt und bewusst.“

30.09.2019 _____

Datum Unterschrift

Ausführliche Anteilserklärung

Publikation 1: Amberg R., Elad A., Beuer F., Vogt C., Bode J., Witte F., Effect of physical cues of altered extract media from biodegradable magnesium implants on human gingival fibroblasts, Acta Biomaterialia, July 2019.

Beitrag im Einzelnen:

Aus der eigenständigen Entwicklung und praktischen Durchführung des Migrationsassays sowie der anschließenden Auswertung sind die Abbildungen 1, 4A, 4D, 4G, 5A, 6A und 7A entstanden. Aus der von mir durchgeführten und ausgewerteten zytotoxischen Assays (MTT, BrdU) sind die Abbildungen 4B, 4C, 4E, 4F, 4H, 4I, 5B, 5C, 6B, 6D, 6F, 7B und 7C entstanden. Die in Abbildung 2C, 6C, 6E und 7D dargestellten Wasserstoffkonzentrationen wurden von mir gemessen und ausgewertet. Die Calcium- und Magnesium-Konzentrationen wurden von Julia Bode an der Technischen Universität Bergakademie in Freiberg durchgeführt und die Abbildungen 2A, 2B, 3, 7E und 7F von mir graphisch dargestellt. Alle statischen Auswertungen wurden von mir durchgeführt und vom Institut für Biometrie der Charité Berlin geprüft. Die Publikation wurde von mir verfasst und von Prof. Dr. Frank Witte überarbeitet. Alle Autoren lasen und genehmigten das finale Manuskript. Die Autoren des Artikels hatten die volle Kontrolle und Handhabe über die Datenanalyse und Interpretation.

_____

Unterschrift der Doktorandin

Curriculum Vitae

Mein Lebenslauf wird aus datenschutzrechtlichen Gründen in der elektronischen Version meiner Arbeit nicht veröffentlicht. (1)

Mein Lebenslauf wird aus datenschutzrechtlichen Gründen in der elektronischen Version meiner Arbeit nicht veröffentlicht. (2)

List of Publications

Amberg R., Elad A., Rothamel D., Fienitz T., Szakacs G., Heilmann S., Witte F., Design of a migration assay for human gingival fibroblasts on biodegradable magnesium surfaces, Acta Biomaterialia, October 2018.

Amberg R., Elad A., Beuer F., Vogt C., Bode J., Witte F., Effect of physical cues of altered extract media from biodegradable magnesium implants on human gingival fibroblasts, Acta Biomaterialia, July 2019.

Acknowledgement

I would like to express my sincere gratitude to my first supervisor, Prof. Dr. Frank Witte, for the continuous support, motivation, patience and immense knowledge during the completion of my PhD and related research. Furthermore, I would like to thank my second supervisor, Prof. Dr. Florian Beuer, for his encouragement and practical insights from the clinical perspective, which had given me a deeper understanding of the clinical application of my research. I would also like to thank all members of my working group for the stimulating discussions, their meaningful support and the pleasant working atmosphere. Last but not least, I thank my family: my mother, brother and both sisters for supporting me spiritually throughout writing my thesis.